Fisheries and Oceans Canada | Pêches et Océans Canada
Ecosystems and Oceans Science | Sciences des écosystèmes et des océans

Canadian Science Advisory Secretariat (CSAS)

Research Document 2017/071

National Capital Region

Oceanographic and environmental conditions in the Discovery Islands, British Columbia

P.C. Chandler[1], M.G.G. Foreman[1], M. Ouellet[2], C. Mimeault[3], and J. Wade[3]

[1]Fisheries and Oceans Canada
Institute of Ocean Sciences
9860 West Saanich Road
Sidney, British Columbia, V8L 5T5

[2]Fisheries and Oceans Canada
Marine Environmental Data Section, Ocean Science Branch
200 Kent Street
Ottawa, Ontario, K1A 0E6

[3]Fisheries and Oceans Canada
Aquaculture, Biotechnology and Aquatic Animal Health Science Branch
200 Kent Street
Ottawa, Ontario, K1A 0E6

December 2017

Canada

Foreword

This series documents the scientific basis for the evaluation of aquatic resources and ecosystems in Canada. As such, it addresses the issues of the day in the time frames required and the documents it contains are not intended as definitive statements on the subjects addressed but rather as progress reports on ongoing investigations.

Research documents are produced in the official language in which they are provided to the Secretariat.

Published by:

Fisheries and Oceans Canada
Canadian Science Advisory Secretariat
200 Kent Street
Ottawa ON K1A 0E6

http://www.dfo-mpo.gc.ca/csas-sccs/
csas-sccs@dfo-mpo.gc.ca

ISSN 1919-5044

Correct citation for this publication:

Chandler, P.C., Foreman, M.G.G., Ouellet, M., Mimeault, C., and Wade, J. 2017. Oceanographic and environmental conditions in the Discovery Islands, British Columbia. DFO Can. Sci. Advis. Sec. Res. Doc. 2017/071. viii + 51 p.

TABLE OF CONTENTS

LIST OF FIGURES

LIST OF TABLES

ABSTRACT

This paper describes the oceanographic and environmental conditions in the Discovery Islands area of British Columbia that are relevant to inform assessments of the risks to wild salmon populations due to pathogen transfer from salmon farms located in the Discovery Islands. Consequently, this paper mainly focuses on the oceanographic and environmental conditions expected to affect the persistence and dispersal of pathogens in the marine environment.

The sources of information used to describe the environmental and oceanographic conditions in the Discovery Islands area include data collected from monitoring and research programs carried out by federal and provincial governments, academic institutions, environmental non-governmental agencies, and by Atlantic Salmon farming companies.

The current state of knowledge and associated knowledge gaps for oceanographic conditions such as water temperature, water salinity, dissolved oxygen and water currents in the Discovery Islands are included. Solar radiation and ultraviolet light as well as biota and suspended solids in the region are also reviewed.

The Finite Volume Community Ocean Model (FVCOM) has been applied in the Discovery Islands to simulate the hydrodynamics in areas of aquaculture activities. This paper includes main conclusions from simulations conducted for April and July 2010, comparisons of observations and modelling simulations and representativeness of conditions observed in April and July 2010. Results from the passive particle tracking model used to simulate the trajectories and dispersion of particles in the water column in the Discovery Islands are also included.

Conditions océanographiques et environnementales de la région des îles Discovery de la Colombie-Britannique

RÉSUMÉ

Le présent document décrit les conditions océanographiques et environnementales dans la région des îles Discovery, en Colombie-Britannique, qui doivent servir à orienter les évaluations des risques pour les populations de saumons sauvages en raison du transfert d'agents pathogènes provenant des élevages de saumons situés dans cette région. Par conséquent, le présent document met surtout l'accent sur les conditions océanographiques et environnementales qui devraient influencer la persistance et la dispersion des agents pathogènes dans le milieu marin.

Parmi les sources de renseignements utilisées pour décrire les conditions océanographiques et environnementales dans la région des îles Discovery, mentionnons les données recueillies à partir de programmes de surveillance et de recherche réalisés par les gouvernements fédéral et provinciaux, des établissements d'enseignement, des organisations non gouvernementales de l'environnement, et des entreprises d'élevage du saumon de l'Atlantique.

On y trouve l'état actuel des connaissances et les lacunes de connaissances connexes qui concernent les conditions océanographiques telles que la température de l'eau, la salinité, l'oxygène dissous et les courants d'eau aux îles Discovery. Le rayonnement solaire et la lumière ultraviolette ainsi que le biote et les solides en suspension dans la région sont également examinés.

Le modèle des volumes finis d'océanologie côtière (FVCOM) a été appliqué aux îles Discovery pour simuler l'hydrodynamique dans les secteurs d'activités aquacoles. Le présent document comprend les principales conclusions provenant de simulations réalisées en avril et juillet 2010, des comparaisons d'observations et de simulations de modélisation et la représentativité des conditions observées en avril et en juillet 2010. Les résultats du modèle de suivi des particules passives utilisés pour simuler les trajectoires et la dispersion des particules dans la colonne d'eau aux îles Discovery sont également inclus.

INTRODUCTION

Fisheries and Oceans Canada (DFO) has a regulatory role to ensure the protection of the environment while creating the conditions for the development of an economically, socially and environmentally sustainable aquaculture sector. Restoring funding to support federal ocean science programs to protect the health of fish stocks, to monitor contaminants and pollution in the oceans, and to support responsible and sustainable aquaculture industries in Canada has been identified as a priority of the Minister of Fisheries, Oceans and the Canadian Coast Guard.

It is recognized that there are interactions between aquaculture operations and the environment (Grant and Jones, 2010; Foreman et al., 2015b). One interaction is the risk to wild salmon populations resulting from the potential spread of infectious diseases from Atlantic Salmon (*Salmo salar*) farms in British Columbia (BC) (Cohen, 2012). While several Atlantic Salmon farms are located within the migratory routes of Pacific salmon species, no risk assessment has been conducted to specifically determine the risk to wild fish populations associated with pathogens released from Atlantic Salmon farms.

DFO Aquaculture Management Directorate requested formal science advice on the risks of pathogen transfer from Atlantic Salmon farms to wild fish populations in BC. Given the complexity of interactions among pathogens, hosts and the environment, DFO will deliver the science advice through a series of pathogen-specific risk assessments followed by a synthesis.

PURPOSE OF THIS DOCUMENT

This document describes oceanographic and environmental conditions in the Discovery Islands area of BC to assist in assessments of the risk to Fraser River Sockeye Salmon due to pathogen transfer from Atlantic Salmon farms located in the Discovery Islands. It includes a state of knowledge, and any associated gaps, of the oceanographic and environmental conditions relevant to understanding the fate of pathogens, including their transport and dispersal away from fish farms in the Discovery Islands area, and conditions that affect the health and physiology of fish species.

Environmental conditions expected to affect survival and dispersal of pathogens in an aquatic environment include temperature, salinity, water currents and geography, ultraviolet light, pressure, biota, contaminants and sedimentation (Grant and Jones, 2010; Garver et al., 2013). Additionally, temperature, photoperiod, dissolved oxygen, suspended solids, salinity, pH and contaminants can impact fish health and/or physiology (reviewed in Grant and Jones (2010)).

Prior to the Discovery Islands region being used for salmon aquaculture, the relatively few oceanographic observations in the region were a result of research into coastal processes. Over the past several years, directed monitoring programs in support of aquaculture operations and aquaculture research have been carried out, and continue to be undertaken. Sources of information used to describe the environmental and oceanographic conditions in the Discovery Islands area therefore include data collected from monitoring and research programs carried out by federal and provincial governments, academic institutions, environmental non-governmental agencies, and by Atlantic Salmon farming companies. Data and details used to support this summary are included in appendices. This report includes both available oceanographic and atmospheric observations and the application of hydrodynamic and particle tracking models.

PHYSICAL SETTING

The Discovery Islands region is at the northern end of the Strait of Georgia, between mainland BC and Vancouver Island. The large-scale physical setting of the Discovery Islands region is defined by tectonic forces that have formed, and continue to shape the west coast of Canada. The coastal mountain ranges have experienced repeated advance and retreat of glaciers carving deep fjords, some with shallow sills, which control the sedimentary input to the coastal waters, and the freshwater input from precipitation and snowmelt to the marine environment (Thomson, 1981). The physical and biological processes in each fjord are a complex interaction of the fresh water input, marine forcing, topography and bathymetry.

The position of the Discovery Islands relative to Vancouver Island and the North Pacific Ocean results in the very strong tidal currents that characterize the area. As the ocean tidal wave travels northwards off Vancouver Island it forces water to flood into the Juan de Fuca Strait and north through the Strait of Georgia. This water flow is met by tidal currents flooding south from Queen Charlotte Strait as the tidal wave continues to propagate northward along the outer coasts of BC. The forcing of water through the network of narrow, twisting channels in the Discovery Islands region contributes to strong semi-diurnal tidal currents that reverse direction every six hours.

Figure 1 shows the Discovery Island region and the names and locations of the 18 Atlantic Salmon farms holding valid marine finfish aquaculture licences for 2015-2016 and having produced Atlantic Salmon at least once since 2010. The western side of the Discovery Islands region has two connecting narrow passages; Johnstone Strait and Discovery Passage, which serve as the primary waterway for commercial marine traffic. The eastern side consists of several inlets and arms with narrow, steep sides and multiple sources of fresh water from streams and rivers. There are three cross-connecting channels that are oriented roughly east-west; Cordero, Nodales, and Okisollo, where most of the fish farms are located.

Figure 2 shows the bathymetry in the Discovery Islands region, and the major islands in the archipelago. With an average of 173 m, water depth varies considerably across the Discovery Islands reaching a maximum of 700 m in Bute Inlet and Homfray Channel (Foreman et al., 2012). Also shown are the locations of the fish farms, which are sited close to shore in water depths ranging from 29 to 158 m.

The circulation of water within the Discovery Islands region, and by extension the particles (including pathogens) transported by water, is controlled directly by the physical constraints imposed by the bathymetry, and indirectly by the influence bathymetry has on the forces that drive the water flow. As a result, there are some areas that are well flushed within hours and others where the residence time can be lengthened due to reduced flushing. The location of these areas varies both by season and on shorter time scales due to wind events, such that both monitoring programs as well as hydrodynamic modelling are required to describe the complex water circulation of the Discovery Islands region.

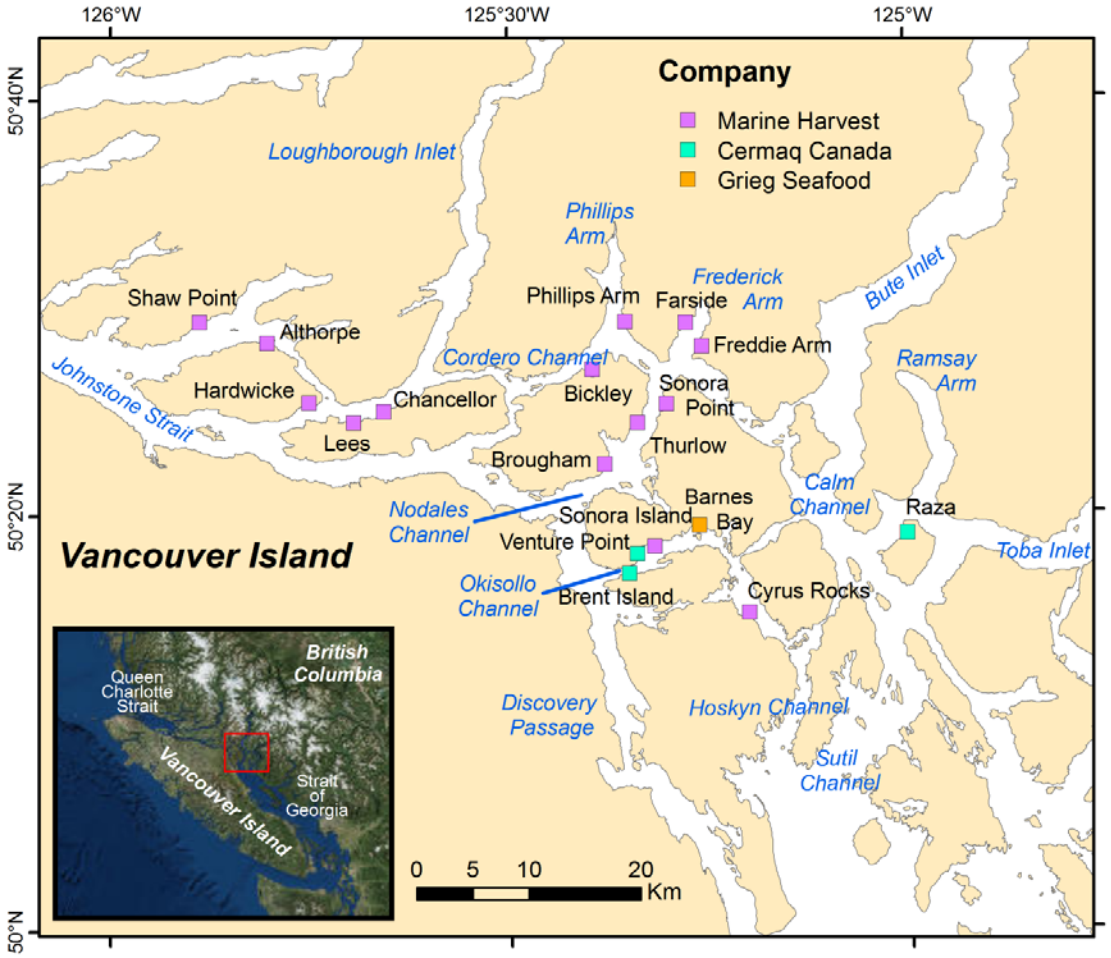

Figure 1. Atlantic Salmon fish farms and place names of significant waterways in the Discovery Islands. The size of the symbol for fish farms does not represent the actual size of the farm.

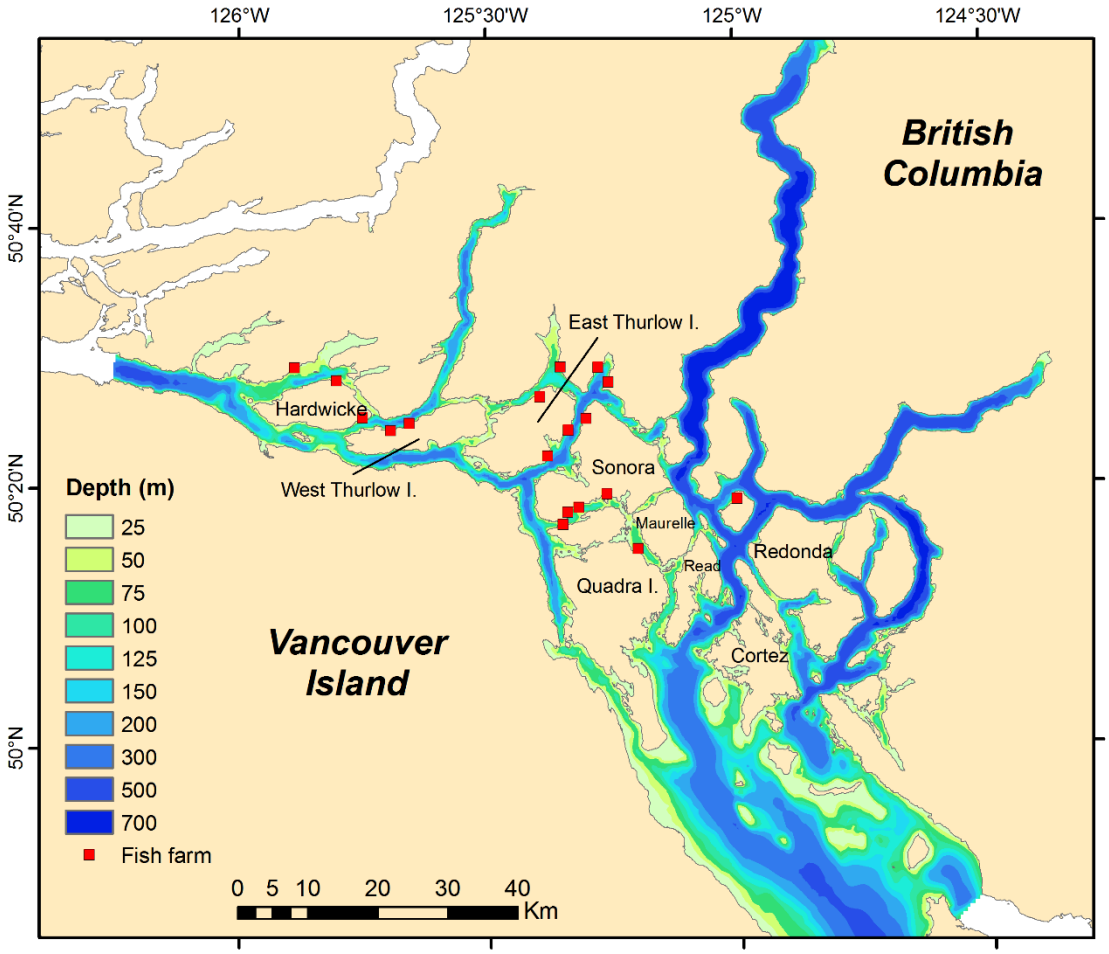

Figure 2. Colour contours of bottom depth for the Discovery Islands area based on bathymetric data provided by the Canadian Hydrographic Service. Adapted from Foreman et al. (2012).

OCEANOGRAPHIC CONDITIONS

TEMPERATURE, SALINITY AND OXYGEN

The early oceanographic data collected in the Discovery Islands area included water sampled in bottles, with temperature measured using glass thermometers, and salinity and oxygen by laboratory titration. The development of electronic sensors in the 1960s provided the ability to accurately measure temperature, conductivity and pressure at a high sampling rate with an instrument that could be lowered through the water column. These data are used to produce conductivity, temperature and depth (CTD) profiles and provide much of the temperature and salinity information for the Discovery Islands.

The national archive of CTD profiles is administered by the Marine Environmental Data Section (MEDS) of the Ocean Sciences Branch of DFO in Ottawa. Significant contributions to this archive have been made by DFO research programs, the University of British Columbia's Inlets program, and the Royal Canadian Navy (previously the Canadian Armed Forces' Maritime Command).

The Canadian Hydrographic Service (CHS) deployed several moorings in the Discovery Islands region (1973-1978, 1987-1988) that were instrumented with temperature and salinity sensors, providing information at a specific location and depth over time periods of several months. Other moorings (2008-2014) were deployed by the Ocean Sciences Division of the Institute of Ocean Sciences (DFO).

The British Columbia Salmon Farmers' Association (BCSFA) maintains a database which includes daily environmental observations collected on Atlantic Salmon farms and includes temperature, salinity and dissolved oxygen at different depths to a maximum of 15 m. The BCSFA provided these data collected between 2005 and 2015 under a data sharing agreement. Consequently, farm data are presented without specifying farm location.

Appendix A provides tables of temperature, salinity and oxygen data referred to in the main report. Because there are several units used to report salinity, a brief review of these are given in Appendix B. Appendix C provides greater detail about the oceanographic archives and databases used in this report.

Figure 3 shows the locations of CTD profiles collected between 1932 and 2015; colour coded by locations determined based on temperature, salinity and oxygen properties of the water. Also shown are the positions of the moorings that provided temperature and salinity information.

CTD data shown in Figure 3 were grouped into nine regions based on the similarity of their physical properties, their connectedness, and the amount of data available. The regions with most of the fish farms (Western Channels (8), Northwestern Channels (5), and Phillips and Fredrick Arms and Cordero Channel (4)) have fewer CTD profiles but the BCSFA database provides good coverage of water properties in these regions. The BCSFA database has been accepted without information on the quality control applied to the data. Further work to harmonize this dataset with the MEDS archive is recommended.

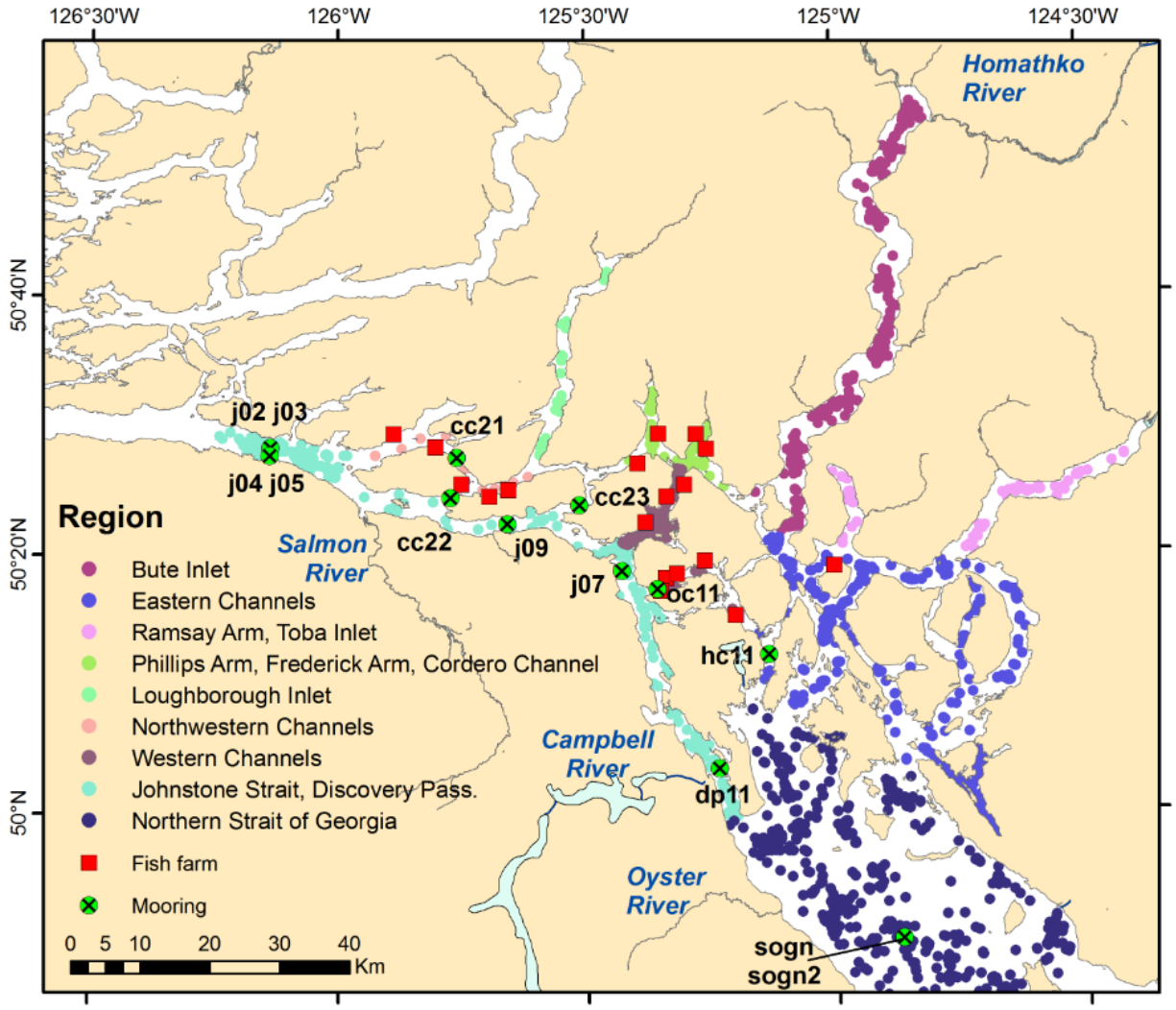

Figure 3. Map of the Discovery Islands showing regions based on geographical and water properties (salinity, temperature and oxygen). Data derived from DFO oceanographic archives (1932 – 2015). Dots represent location of oceanographic profiles and crosses within circles represent location of moored temperature and salinity records. Alphanumeric codes are associated with oceanographic moorings (see Table 1).

Spatial and temporal variations

Temperature

Water temperature in the Discovery Islands varies both spatially (by region and through the water column) and seasonally. Figure 4 shows water temperature data for each of the nine regions in depth ranges 0-30 m and 30-60 m. While there are differences in the number of observations for each region it can be seen that the greatest temperature variability occurs in the upper 30 m. The maximum near surface temperature values are usually observed between June and August, and in spring and summer the upper waters in the Eastern channels are warmer (>20ºC) than those of the Western channels (<15ºC). There is less spatial variability in the lower winter temperatures, and the coldest temperatures are observed in the inlets, Eastern channels and Northern Strait of Georgia.

Monthly average temperature across the Discovery Islands regions ranges from 6 to 14ºC, with minimum and maximum of 3 and 24ºC, respectively. Monthly average temperature among the Discovery Islands regions varies between 6 and 8ºC in the winter and 10 and 14ºC in the summer (see Table 7 for more details).

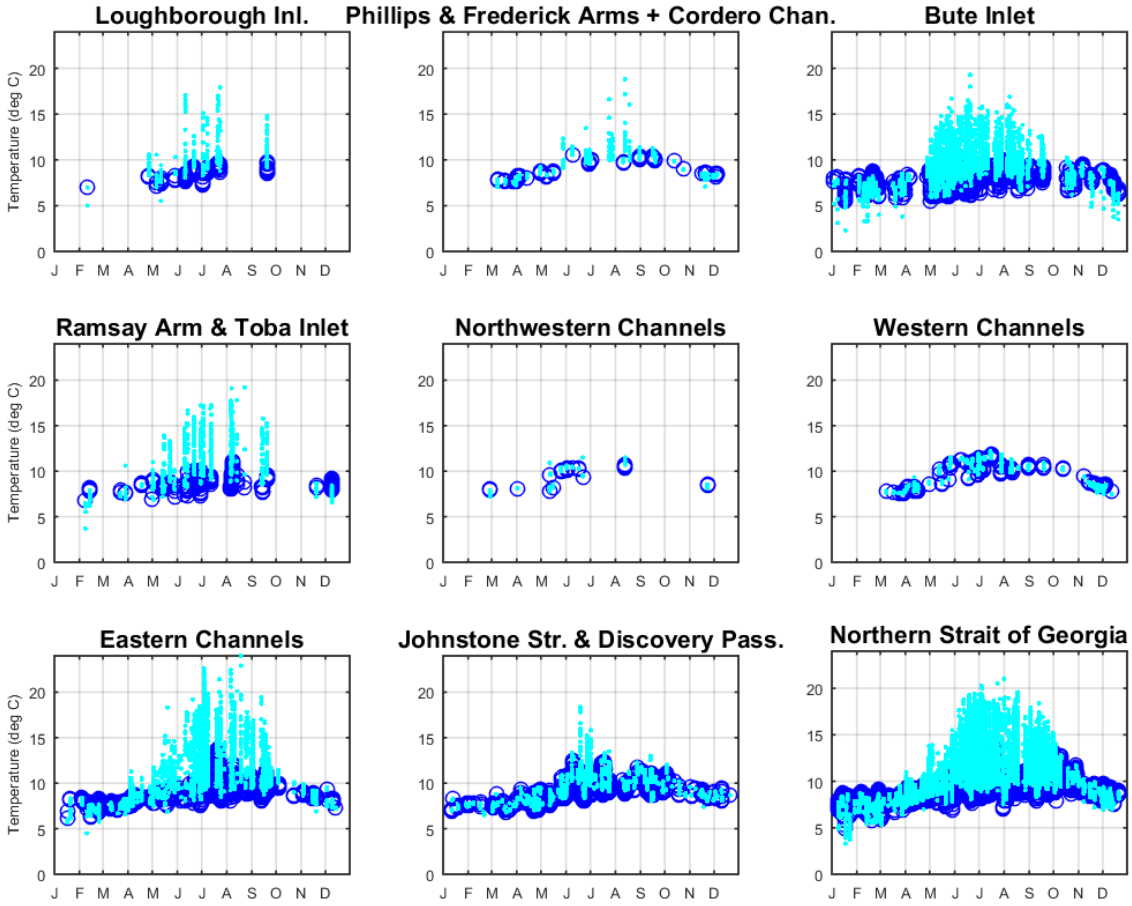

Figure 4. Water temperature observations between 0 and 30 m (light blue dots) and 30 to 60 m depth (dark blue open circles) in different regions of the Discovery Islands plotted by day of year. Observations between 30 and 60 meters were plotted first followed by observations between 0 and 30 m. Points represent individual temperature observations collected between 1932 and 2015 (Appendix C). Average, range and number of observations and profiles from which they were gathered are provided in Table 7.

The combined water temperature data collected at fish farms in the Discovery Islands between August 2001 and November 2015 are shown in Figure 5. These data represent conditions in the Western channels, Northwestern channels, Cordero Channel, and Phillips and Fredrick arms at three depths: surface (between 0 and 5 m), 10 m, and 15 m. Water temperature on fish farms follows a seasonal cycle with coldest and warmest average temperatures reported in February and August, respectively (Figure 5).

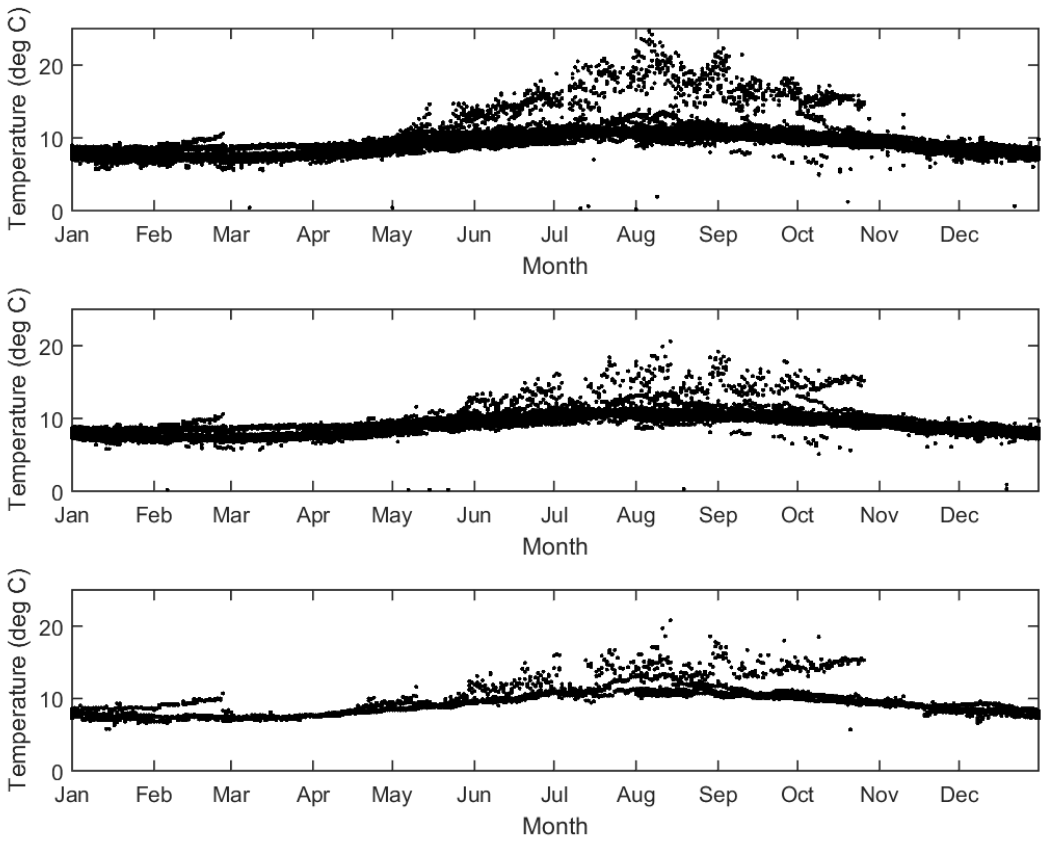

Figure 5. Water temperature observed on Atlantic Salmon farms located in the Discovery Islands. Each dot represents an observation collected between 0 and 5 meters (top panel, n=11,577), at 10 meters (middle panel n=11,563) or at 15 meters (bottom panel n=4,396) between August 2011 and November 2015.

Figure 6 shows the vertical distribution of temperature from data collected using bottles and profiling instruments in the nine regions and demonstrates that most of the variability occurs in the top 30 m. The magnitude of variation is also seen to vary with season and region, though dependent on the number of samples (see Table 7). As noted by Thomson (1981) and shown on Figure 6, the waters of Johnstone Strait and Discovery Passage become uniformly cold from top to bottom during winter but warmer waters near the surface are sometimes observed in the spring and summer. The Northwestern and Western channels are the only regions where there are no observations showing warmer water near the surface than deeper in the water column.

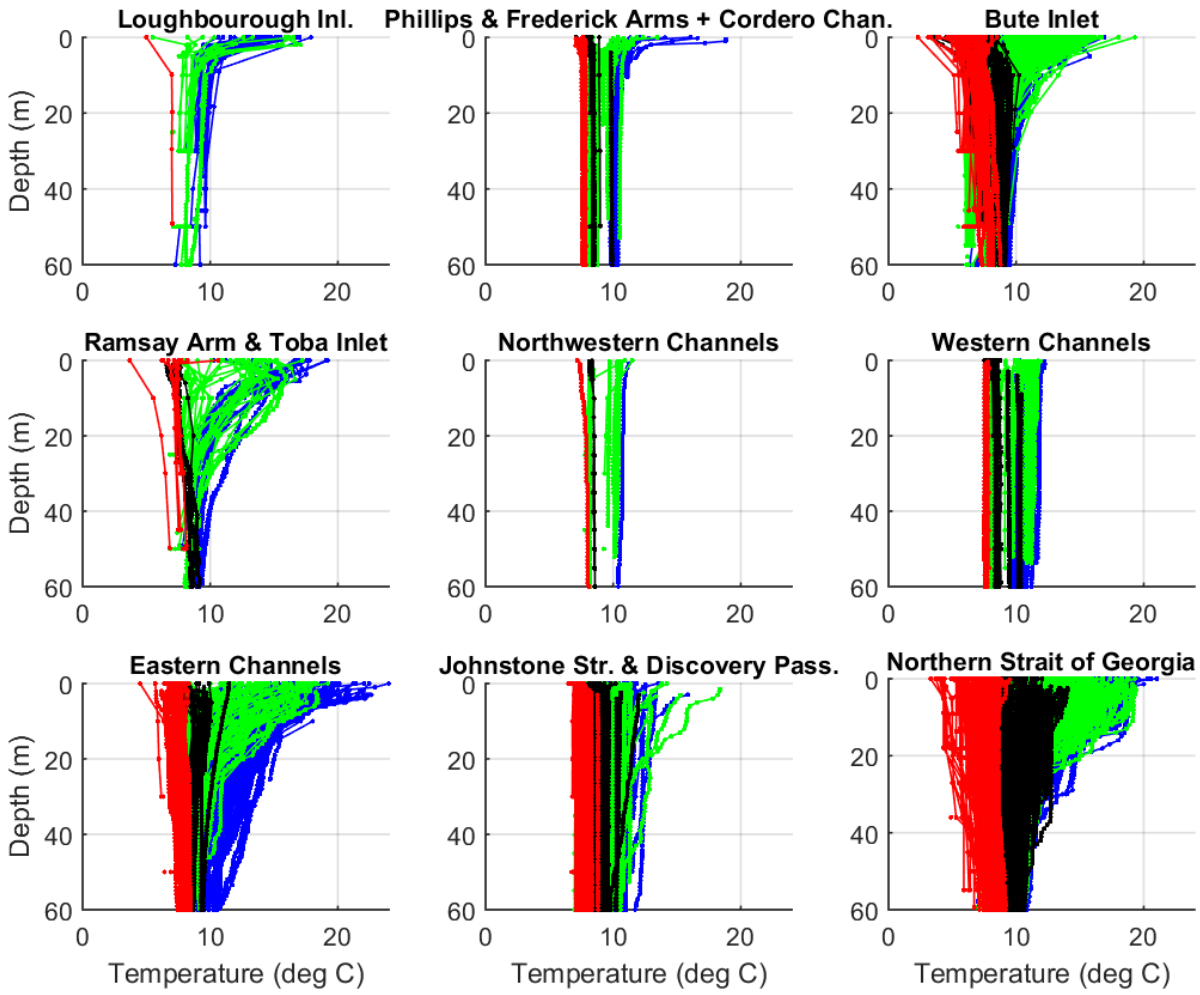

Figure 6. Vertical distribution of temperature in the nine regions of the Discovery Islands from oceanographic profiles collected between 1932 and 2015. Observations were plotted sequentially starting with summer (July to September) in blue, spring (April to June) in green, autumn (October to December) in black and winter (January to March) in red. The number of profiles and observations is provided in Table 4 (Appendix B). Continuous lines are only drawn between vertical values separated by 20 m (or 20 dbar) or less.

Snapshots of sea surface temperature have been acquired using satellite imagery such as LANDSAT with thermal infrared remote sensors (Lim et al., 2015). LANDSAT sensors provide a spatial resolution ranging from 60 m to 120 m, but coverage is often reduced by cloud cover. The imagery is a potentially useful tool for validating the spatial sea surface temperature patterns generated by high resolution hydrodynamic models such as FVCOM, but this has yet to be done for the Discovery Islands region.

Salinity

The vertical distribution of temperature and salinity determines the density of the water column which defines the stratification and the extent of mixing. The likelihood of pathogens introduced near the surface to be mixed deeper into the water column, or to remain trapped within the surface layer, are factors that control the concentration and infectivity of the pathogen.

Water salinity in the Discovery Islands varies both spatially, by region and through the water column, and seasonally. In the Discovery Islands region, the salinity varies with the amount of fresh water from direct precipitation and river runoff. There is a rainy season during the winter months, and river runoff regulated by the melting snowpack and glaciers is high in spring and summer.

Figure 7 shows the salinity profiles associated with the temperature data given in Figure 4 (these CTD data have the same temporal and spatial distribution). The influence of the reduced salinity due to snowmelt can be seen in the spring profiles for the inlets and arms on the eastern side of the Discovery Islands. Bute Inlet is supplied by fresh water from the Homathko River which has a peak discharge in July exceeding, on average, 600 $m^3 s^{-1}$. Below about 15-20 m the salinity of Bute Inlet does not change much with depth and this represents the depth of the surface layer. By comparison, Johnstone Strait and Discovery Passage to the west show little variation in salinity with depth, and this lack of stratification reveals a well-mixed water column which is due to the vigorous tidal mixing that takes place over the sills and in the narrow passes (Thomson, 1981).

Monthly average salinity across the Discovery Islands regions ranges from 23 to 31, with a measured minimum close to zero and a maximum of 32. Monthly average salinity among the Discovery Islands regions varies between 27 and 30 in the winter and 23 and 31 in the summer (see Table 8 for more details).

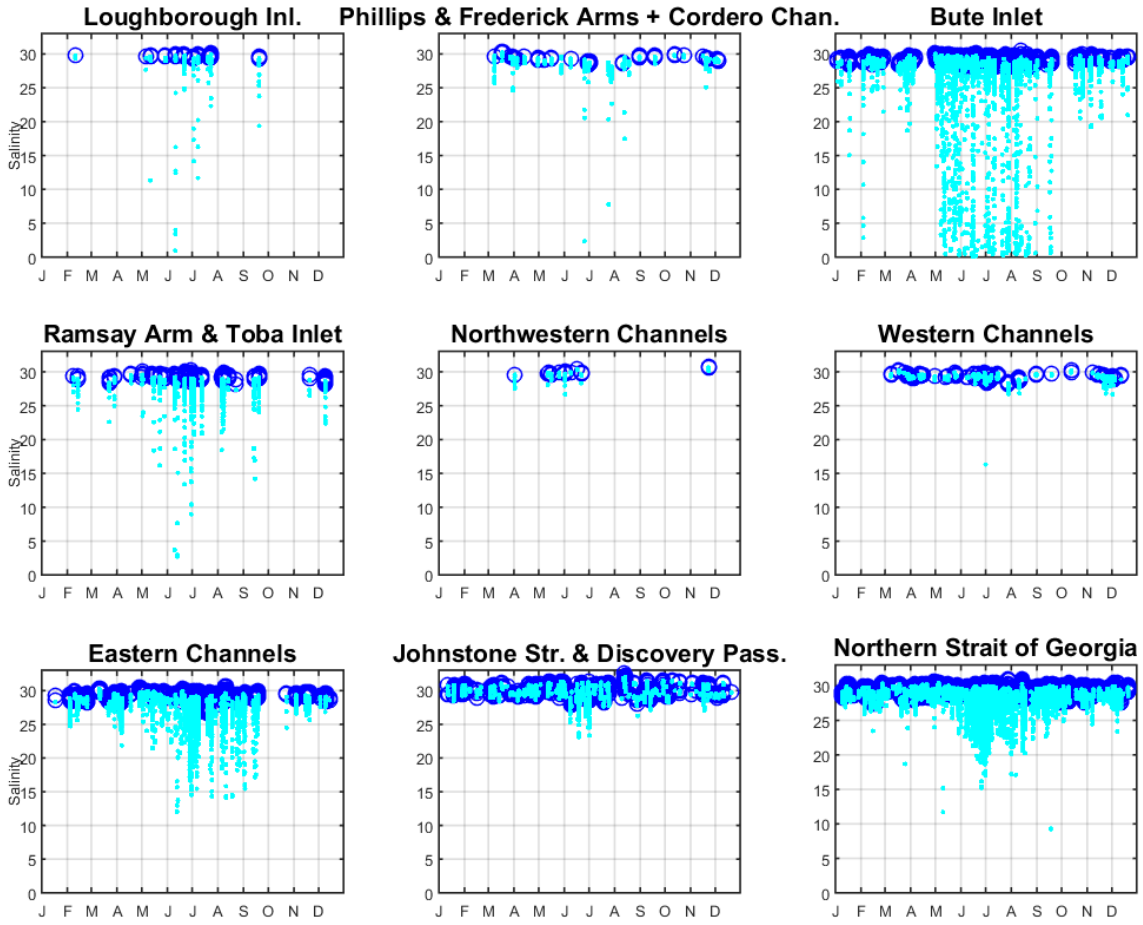

Figure 7. Water salinity (blend of data in PSS-78 and g kg^{-1} equivalent units for historical data; see Appendix B) observed between 0 and 30 m (light blue dots) and 30 to 60 m depth (dark blue open circles) in different regions of the Discovery Islands. Observations between 30 and 60 m were plotted first followed by observations collected between 0 and 30 m. Points represent individual salinity observations collected between 1932 and 2015 from various sources (see Appendix C). Average, range and number of observations and profiles from which they were gathered are described in Table 8.

The gaps in CTD salinity data for the east-west connecting channels, where most of the fish farms are situated, are supplemented with observations made at the fish farms. Figure 8 shows the combined times series from all fish farms at three depths (between 0 and 5, 10 and 15 m). There is a greater variability in salinity during the summer months due to snowmelt (less than 10 ppt and greater than 30 ppt) at the surface, and a much narrower salinity range at depth (also seen in Figure 7). The narrower salinity range at 15 m for the first part of the year seen in Figure 8 suggests a shallower surface layer during this period.

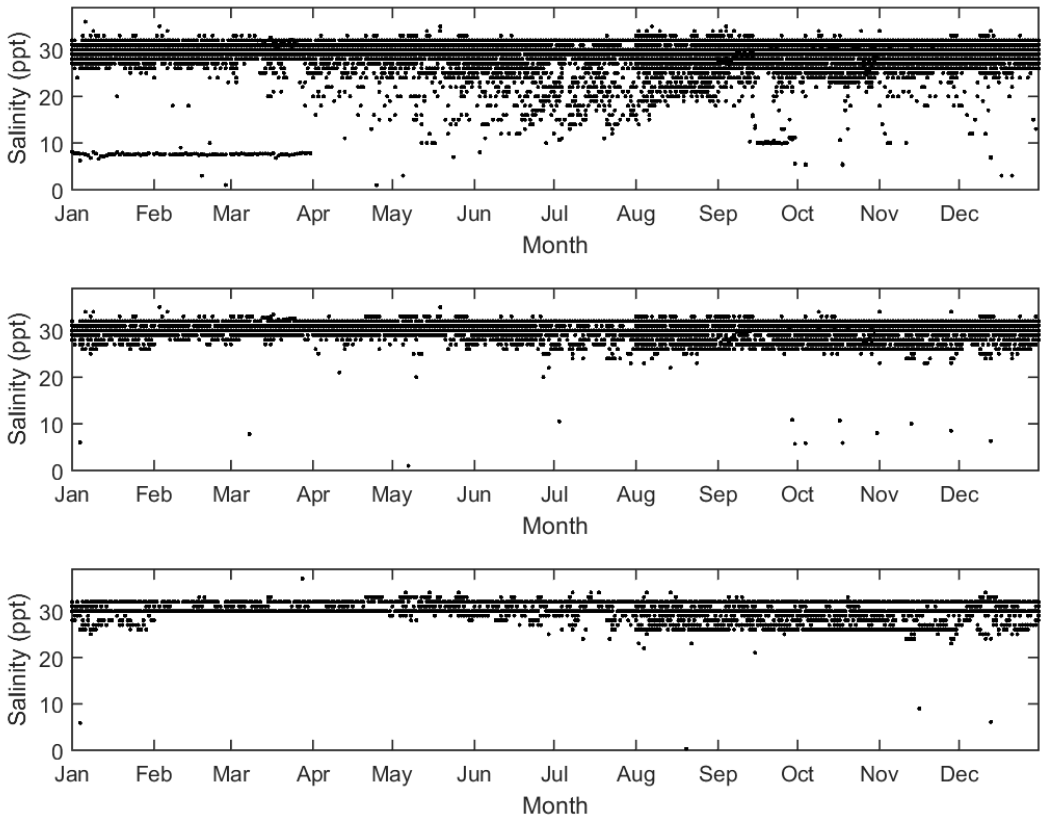

Figure 8. Water salinity observed on Atlantic Salmon farms located in the east-west connecting channels of the Discovery Islands. Each dot represents an observation collected between 0 and 5 meters (top panel, n=11,402), at 10 meters (middle panel n=9,754) or at 15 meters (bottom panel n=4,398) between August 2011 and November 2015. Note: in the upper panel the record of salinities with a continuous value of less than 10 ppt is unverified.

Figure 9 shows the vertical distribution of salinity in the nine regions and shows, as in Figure 7, that most of the variability occurs in the top 20 m. The magnitude of variation is seen to vary with season and region, as in Figure 8.

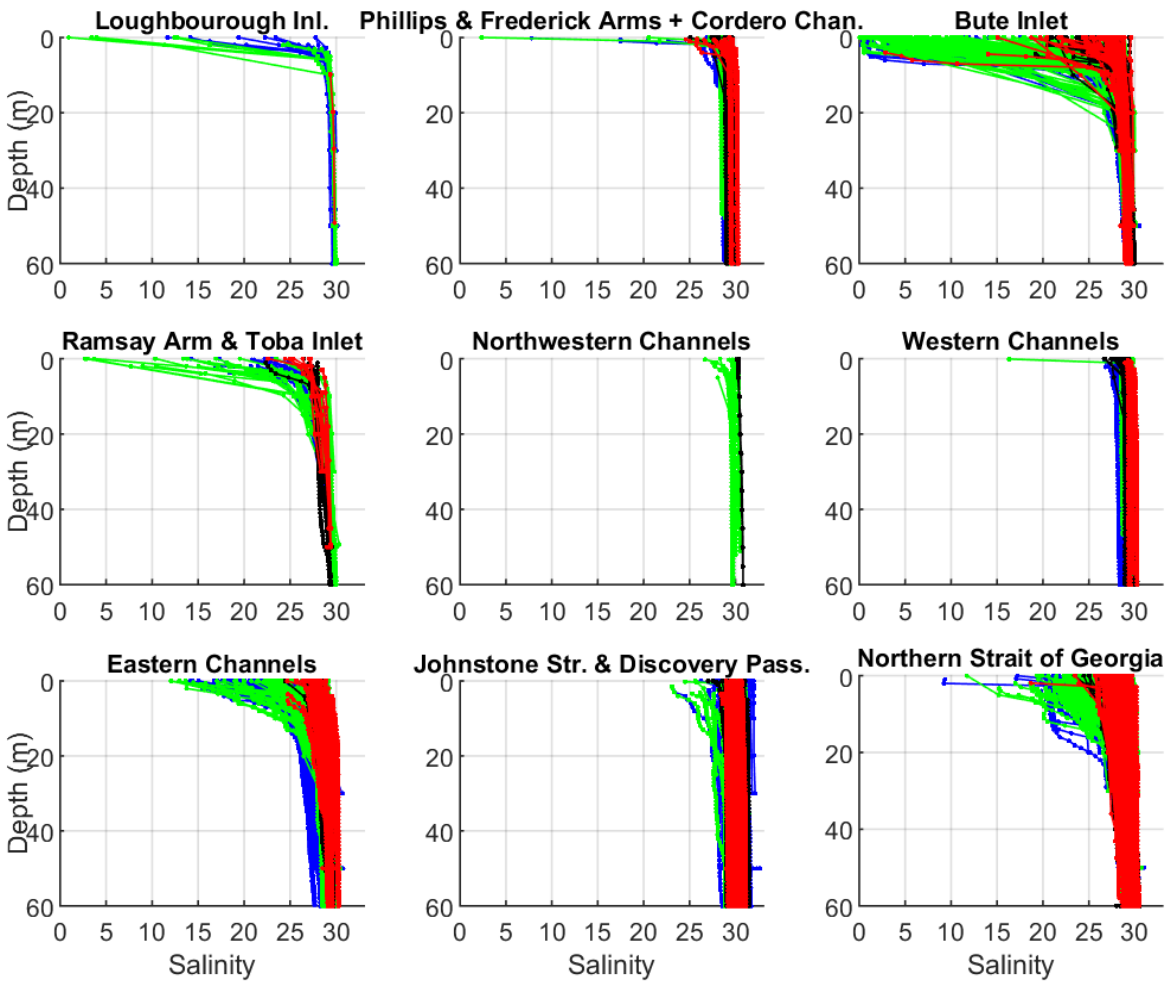

Figure 9. Vertical distribution of salinity in the nine regions from oceanographic profiles (CTD, bottles). Observations were plotted sequentially starting with summer (July to September) in blue, spring (April to June) in green, autumn (October to December) in black and winter (January to March) in red. The number of profiles and observations is provided in Table 5 (Appendix B).

Dissolved oxygen

The concentration of dissolved oxygen in the water has implications for the health and physiology of fish (Grant and Jones, 2010) and while it is not directly relevant to the fate and dispersal of all pathogens, it is a fundamental descriptor of the oceanography of a region.

The level of dissolved oxygen in water can be increased due to diffusion from the atmosphere (which is accelerated during storms and vigorous surface mixing events) and photosynthesis by aquatic plants. Oxygen levels are reduced by respiring fish and animals, and when bacteria and other decomposer organisms consume oxygen. The solubility of oxygen, or its ability to dissolve in water, decreases as the water's temperature and salinity increase. Fish use more oxygen at warmer water temperatures because their metabolic rates increase.

As shown in Figure 2, the fjords in the region are characterized by very deep and narrow channels. Cross-channel sills are a common feature and deep water trapped in the channel between these sills can have very little flushing resulting in very low oxygen levels. Surface waters are generally well oxygenated due to mixing with the atmosphere. The concentration of dissolved oxygen varies both spatially by location and by depth and, temporally by season.

A broad averaging of the oxygen data collected in the Discovery Islands area is given in Figure 10 and shows that dissolved oxygen varies spatially, by region and through the water column, and appears to also vary seasonally. The higher dissolved oxygen concentrations are nearer the surface and occur in the most sampled regions; Northern Strait of Georgia and Eastern channels. Dissolved oxygen values at depth (30-60 m) are similar in all regions. It can be seen that some areas are quite data poor compared to others.

The monthly average levels of dissolved oxygen across the Discovery Islands regions ranges from 170 to 340 mmol m^{-3}, with minimum and maximum of 50 and 550 mmol m^{-3}, respectively. Monthly average levels of dissolved oxygen among the Discovery islands regions varies between 221 and 293 mmol m^{-3} in the winter and 174 and 297 mmol m^{-3} in the summer (see Table 9 for more details).

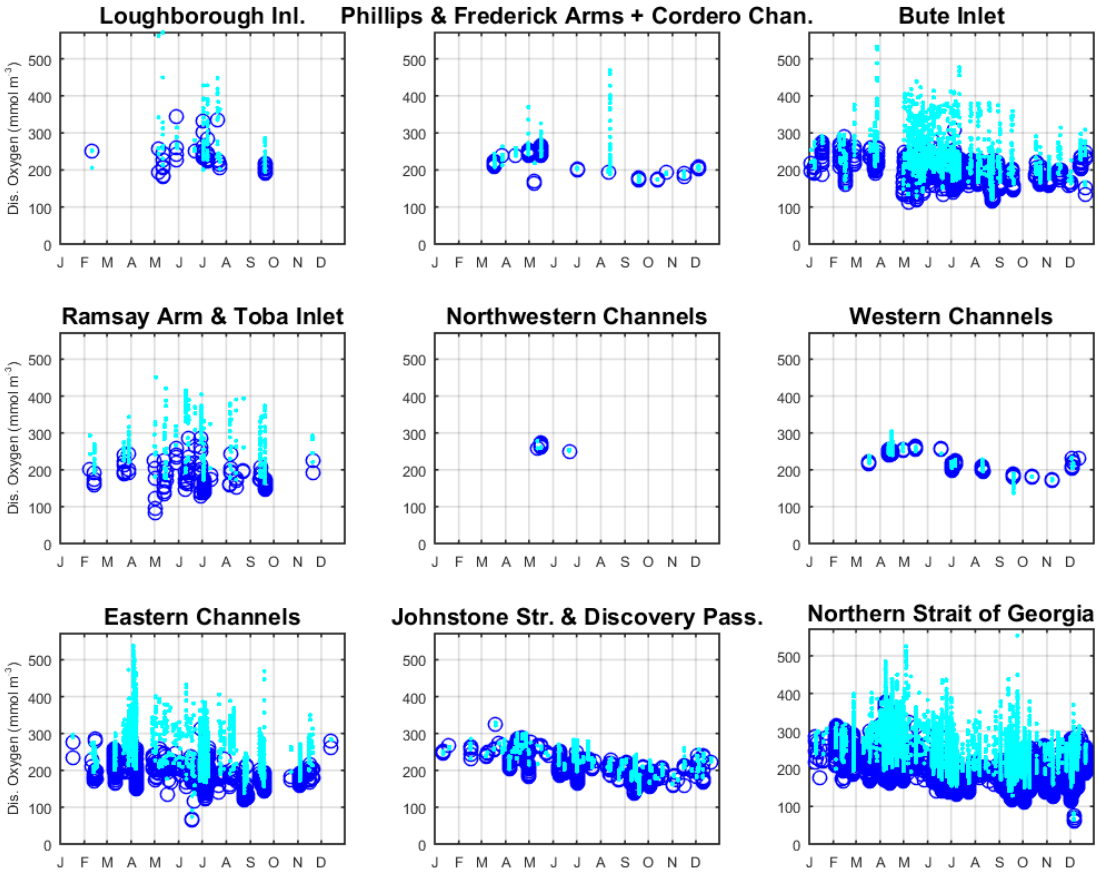

Figure 10. Dissolved oxygen observed between 0 and 30 m (light blue dots) depth and 30 to 60 m (dark blue open circles) depth in different regions of the Discovery Islands. Observations between 30 and 60 m were plotted first followed by observations collected between 0 and 30 m. Points represent individual dissolved oxygen observations collected between 1932 and 2015 from various sources (see Appendix C). Average, range and number of observations and profiles from which they were gathered are described in Table 9.

Observations made at the fish farms at three depths (between 0 and 5, 10 and 15 m) demonstrate a greater variability in dissolved oxygen at the surface (between 0 and 5 m) and a much narrower, and generally lower, range at 15 m (Figure 11).

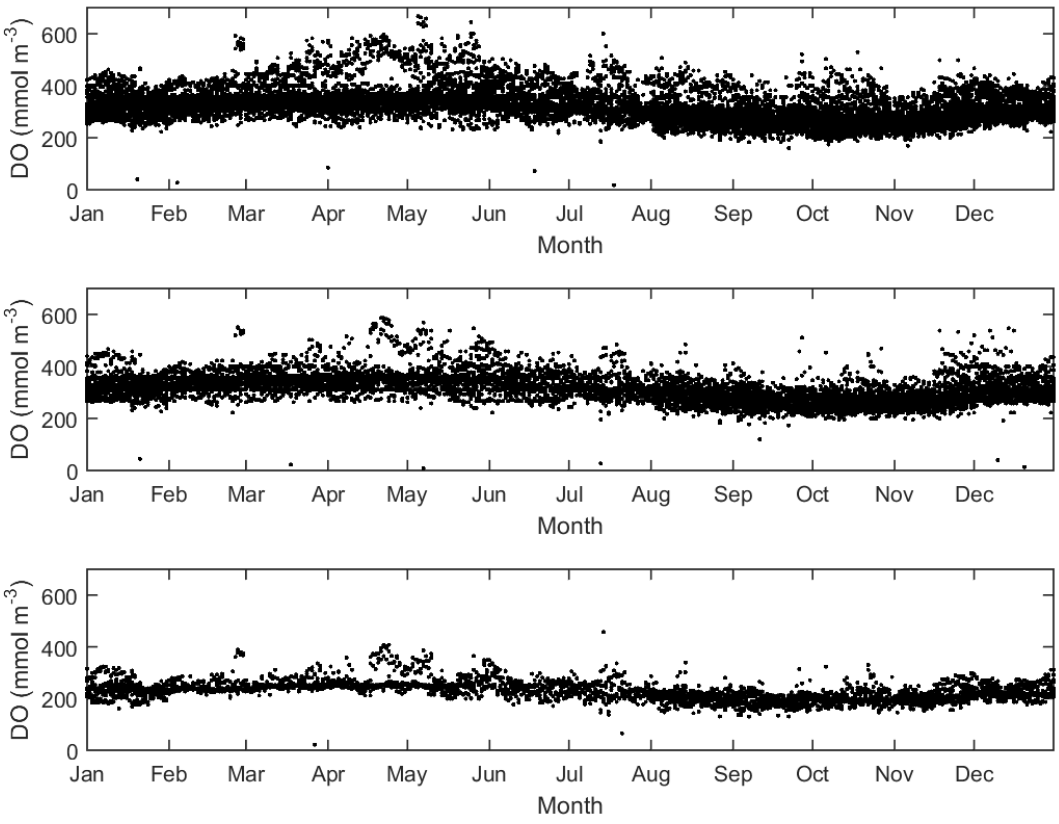

Figure 11. Water dissolved oxygen observed on Atlantic Salmon farms located in the Discovery Islands. Each dot represents an observation collected between 0 and 5 meters (top panel, n=9251), between 6 and 10 meters (middle panel n=9516) or at 15 meters (bottom panel n=4391) between August 2011 and November 2015.

Figure 12 shows the vertical distribution of dissolved oxygen in the nine regions and shows that most of the variability, primarily due to wind mixing, occurs in the top 10 m, consistent with wind mixing and biological activity. The magnitude of variation is seen to vary with season and region.

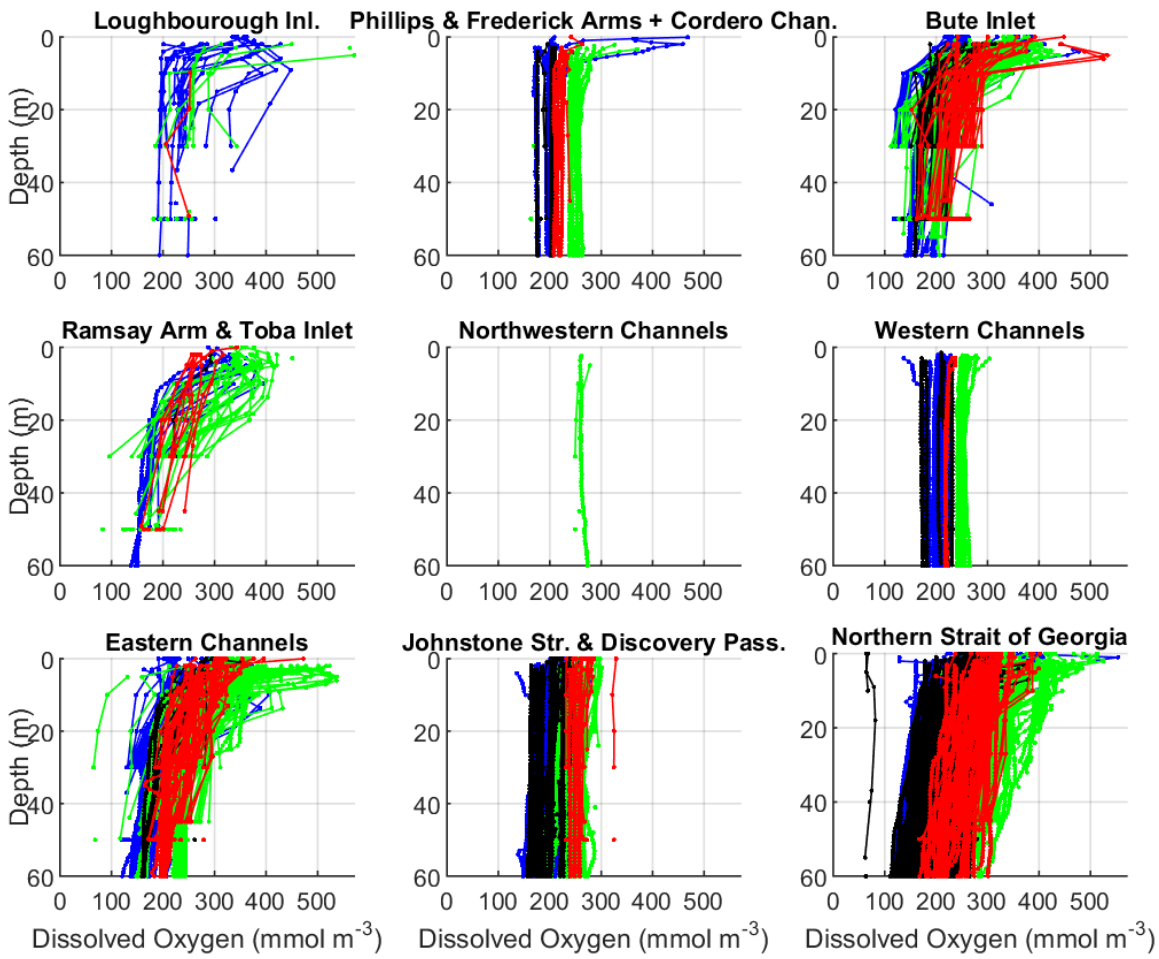

Figure 12. Vertical distribution of dissolved oxygen in the nine regions from oceanographic profiles (CTD, bottles). Observations were plotted sequentially starting with summer (July to September) in blue, spring (April to June) in green, autumn (October to December) in black and winter (January to March) in red. The number of profiles and observations is provided in Table 6 (Appendix B.) Continuous lines are only drawn between vertical values separated by 20 m (or 20 dbar) or less.

Subdiurnal variations

As pathogens introduced into the marine environment can become inactive within days, an understanding of subdiurnal variability (i.e., variations which happen in 24 hours or less), is relevant to pathogen transfer risk assessments. Subdiurnal variations can arise from tides (vertical, horizontal water movements) combined with stratified conditions, as well as changes in atmospheric (wind, temperature, rainfall) conditions.

Data collected at the mooring sites (see Figure 3) provide a time series of temperature and salinity at 30 minute intervals and an insight into the shorter term variability of these conditions. Forty data records from 14 moorings deployed in the Discovery Islands between 1973 and 2014, having at least one instrument above the 60 m depth and with at least 49 days of data, were analyzed. All moorings recorded temperature and six moorings also recorded salinity.

The extreme subdiurnal variations of temperature and salinity (both increases and decreases) calculated from those records are shown in Table 1. On average, the subdiurnal variations are relatively low but under certain environmental conditions, such as a combination of spring tides

and a vertically stratified water column, they can be important. For example, temperature has been observed to vary by as much as 2.3ºC and salinity by as much as 7.3 (PSS-78) in a 24-hour period in the 10 to 26 m depth range in Hoskyn Channel (mooring hc11). Relatively high subdiurnal temperature variations (-3.4ºC) at a depth of 10 m has also been observed in Discovery Passage (mooring dp11). Scrutiny of the data shows that these high subdiurnal changes were followed by similar magnitude changes in the other direction and could be the result of salinity spikes, though the values attained by these spikes are observed elsewhere through the records. No further information on the mooring data quality, configuration or processing were available.

Table 1. Subdiurnal variations calculated from mooring data collected in the Discovery Islands between 1973 and 2014. The depth/pressure range is an indication of the position of the mooring in the water column in dbar units roughly equivalent to meters in depth in the upper 100 m range. A star indicates a nominal depth value when the mooring didn't have a pressure sensor. See Figure 3 for mooring locations.

Region	Mooring	Depth/ Pressure range	Months sampled	Subdiurnal variability				
				# days	Min △T(°C)	Max △T(°C)	Min △S	Max △S
Eastern channels	hc11	10* to 26.3	Jan - Dec	371	-2.4	2.3	-7.3	7.9
	hc11	45* to 59.2	Jan - Dec	371	-1.5	1.7	-2.5	2.6
Johnstone Strait and Discovery Passage	dp11	10*	Apr - Jul	100	-3.4	2.9	-	-
	dp11	22*	Nov - Apr	138	-0.8	1.1	-	-
	j02	75*	Feb - Jun	112	-0.4	0.5	-	-
	j03	15* to 31.7	Jan - Jun	1521	-0.6	0.5	-0.4	0.5
	j03	75*	Feb - Apr	49	-0.1	0.1	-	-
	j04	75*	Feb - Jun	111	-0.4	0.4	-	-
	j05	15* to 55*	Feb - May	86	-0.1	0.4	-	-
	j07	8.4 to 13.4	Mar - May	65	-0.5	0.5	-0.3	0.3
	j09	26.4 to 48.1	Jan - Apr	65	-0.1	0.1	-0.6	0.7
Northern Strait of Georgia	sogn	39.7 to 64.5	Jan - Dec	1579	-1.7	2.2	-0.8	1.6
	sogn2	52*	Feb	135	-1.2	1.1	-	-
Northwestern channels	cc21	10*	Jan - Dec	727	-1.3	1.4	-	-
	cc22	24*	Jan - Dec	385	-0.5	0.5	-	-
	cc23	10*	Jan - Dec	373	-0.4	0.5	-	-
Western channels	oc11	15*	Nov - Apr	127	-0.2	0.2	-	-
	oc11	50*	Nov - Apr	127	-0.2	0.3	-	-

WATER CURRENTS

The Discovery Islands are characterized by fjord-like geography with narrow, steep-sided channels. The strong currents that exist throughout the Discovery Islands have made them difficult to measure using the conventional method of single-depth recording instruments on a taught-line mooring. More recent technology using Acoustic Doppler Current Profiling (ADCP) instruments has started to fill these gaps. Figure 13 shows the locations of nine ADCP moorings deployed between 2009 and 2015. Generally each mooring consisted of two upward-looking instruments, a lower frequency ADCP placed on the bottom and a higher frequency ADCP typically moored at 40-50 m depth to provide better resolution of the upper part of the water column. Each mooring remained in place for one-to-two years and then was moved to a new location. Current data were recovered from near-bottom to near-surface with bin separations (depending on ADCP frequency) varying from two to ten meters.

Currents in the surface layer are particularly relevant to pathogen risk analysis because it is at these depths that juvenile salmon are more likely to be found. Figure 13 shows the average seasonal flow for depths between 9 and 19 m; ADCP data closer to the surface (< 9 m) have not been included as they are often contaminated with acoustic noise generated by surface waves.

Current meter data from moorings located in the northwestern channels of the region show a generally consistent flow at all seasons toward Johnstone Strait; spring and summer data show stronger flow that can be attributed to river runoff. Currents recorded at the more open locations in the northern Strait of Georgia are generally weaker and more affected by wind conditions. For example, SC1 (Sutil Channel) reflects the influence of northwesterly summer winds and the more southerly winter winds. Conditions in Calm Channel (CaC1) appear to combine a strong outward flowing surface current in spring and summer (associated with the freshet from Bute Inlet), and the southerly winter wind driven flow (see Figure 13).

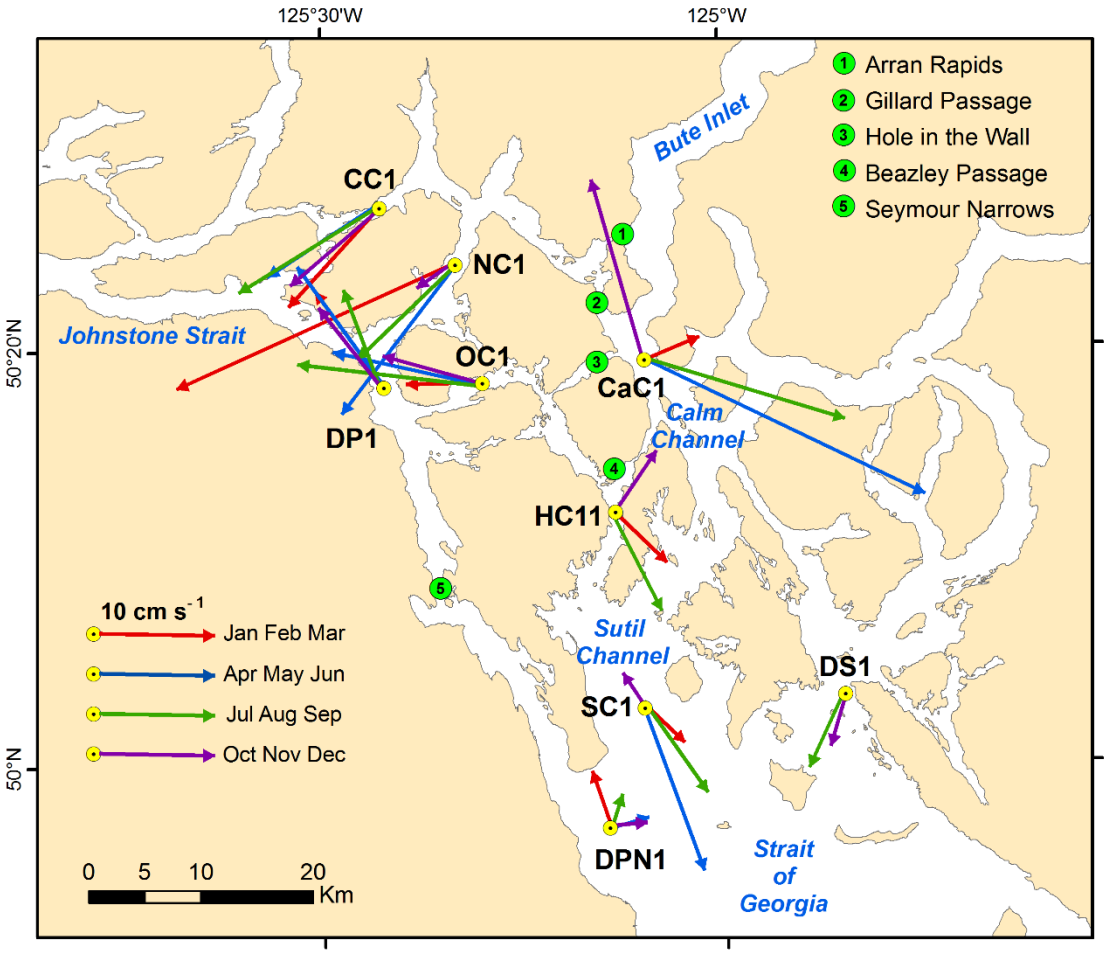

Figure 13. Seasonally-averaged, 9-19 m flows at nine ADCP mooring sites. January-March, April-June, July-September, and October-December values are shown in red, blue, green and yellow, respectively. Green dots show the sites of CHS tide table current data.

The movement of the water in the Discovery Islands region is controlled primarily by three components: tidal currents, buoyancy currents (often referred to as estuarine flows and which

are primarily due to freshwater inputs) and wind-driven currents (surface forcing and subsequent mixing during strong winds).

Tidal currents

Tidal processes are major energetic contributors to the water currents (Tinis and Thomson, 2004) and some of the strongest tidal currents in the world (7.8 m s^{-1} in Discovery Passage, Lin et al. (2011)) are found in the Discovery Island area (Foreman et al., 2015a). This strength is due to the tides arriving from the south (Strait of Georgia) having a timing that differs by several hours from those arriving from the north (Queen Charlotte Strait). In general, ebb currents (flowing to the north) are stronger than flood currents and there are variations over a 15 day period (the spring-neap cycle).

Tidal streams in Queen Charlotte Strait and the Strait of Georgia are generally weaker than in the constricted regions of Johnstone Strait and Discovery Passage. Currents in the interconnecting channels (where most fish farms are located) are localised depending on small scale geography and bathymetry in the area.

Tidal currents can move particles back and forth in a given area due to the six hour reversal of direction from flood and ebb flows. The length scale of these excursions depends on the current velocity, for example a 12.4 hour tidal current of 1 m s^{-1} can transport water over 14 km in one direction until the tide changes. However, when tidal current gradients are strong, as is the case for many areas in the Discovery Islands, tidal currents can also contribute to the net transport of particles over several tens of kilometres.

The transport of pathogens on short time and length scales can be dominated by the tides. A summary of the tidal amplitudes at the major tidal frequencies for five locations (see Figure 13) used in the Canadian Tide and Current Tables is given in Table 2.

Table 2. Along-channel amplitudes (cm s^{-1}) of the two major tidal constituents at five locations (Figure 13) in the Discovery Islands region. Data source Canadian Hydrographic Service.

Locations	M_2	K_1
Arran Rapids	456	99
Beazley Passage	369	78
Gillard Passage	356	82
Hole-in-the-Wall	373	79
Seymour Narrows	466	101

Buoyancy currents

The force of gravity on water with differences in density generates water movement known as buoyancy currents. Thermal heating by the sun has some influence on buoyancy but in the Discovery Islands region the density differences are primarily due to changes in salinity, particularly from freshwater introduced to the system by river runoff.

Figure 3 shows there are numerous streams and creeks that contribute to the fresh water flux into the marine environment of the Discovery Islands, but the water flow at only four of these are gauged; the Homathko, Salmon, Oyster, and Campbell rivers. Discharge data for the first three rivers are available from Water Survey of Canada (Environment and Climate Change Canada (ECCC)) while the latter, because it is regulated by several dams, can be estimated from BC Hydro data.

Figure 14 shows the monthly mean discharge rate for the first three rivers. The greatest annual average discharge is from the Homathko River with 259 $m^3 s^{-1}$, compared to the Salmon River at 61 $m^3 s^{-1}$ and the Oyster River at 13 $m^3 s^{-1}$. The difference in the seasonal cycle is also clear with the Homathko River being dominated by a snowmelt runoff that peaks in July, and the other two Vancouver Island rivers showing greater flow in the winter in response to precipitation.

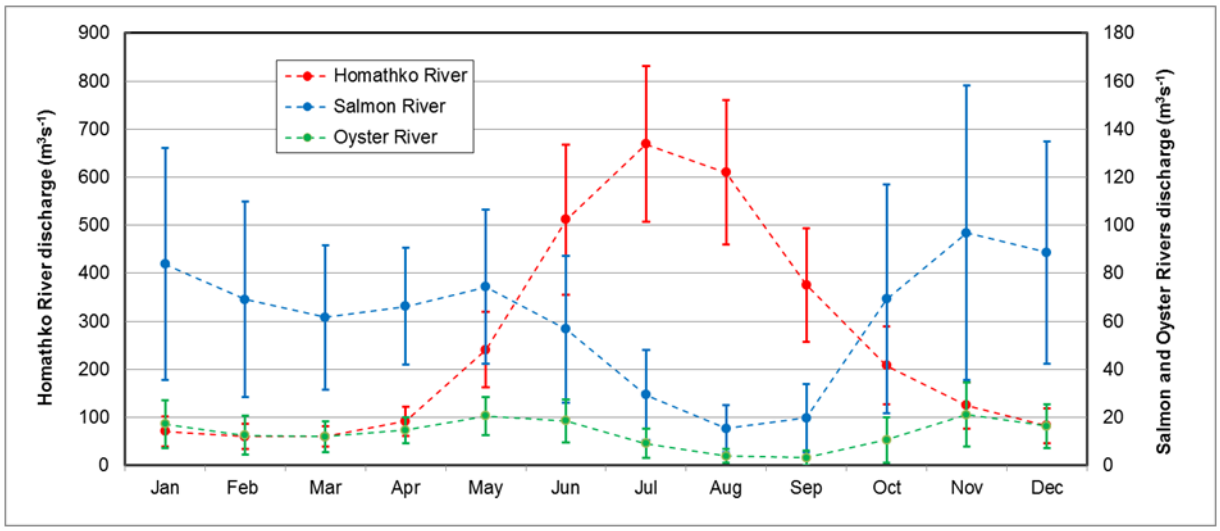

Figure 14. Monthly average discharge for the Homathko (1957 to 2012), Oyster (1974 to 2012) and Salmon (1957 to 2012) rivers in the Discovery Island area, BC. Note the different vertical scaling. Data source: the Water Survey of Canada (ECCC, 2015).

At the river mouth the momentum of the water will contribute to a local current, but the large scale circulation is more influenced by the density differences between the fresher surface layer and the saltier water below. In general, an estuarine circulation is established as gravity pulls the fresher surface water seaward and a return of saltier water occurs at depth. Vertical stratification and mixing will determine the strength and depth of these currents. In Discovery Passage, for example, the water layer in the top 100 m flows northward, on average, while the layer below 100 m flows southward (Thomson, 1981).

Wind driven currents

Situated between the Coast Mountains and the northeast Pacific Ocean the large scale meteorology in this area is dominated by the Aleutian Low Pressure system (winds from the southeast) in winter and the North Pacific High (winds from the northwest) in summer. These winds are modified at smaller scales by the passage of storm fronts, coastal lows, and Arctic outflow conditions. The steep sided topography characteristic of fjords, determines the strength and direction of local winds by steering them along channel. The wind stress exerted on the water surface transfers momentum to produce a wind driven current in proportion to the strength of the wind (typically about 3% of the wind speed).

The topographic complexity of the Discovery Island region means that the wind field at any given location is very site specific. In general, winds will flow along channel, but changes in channel direction will setup cross channel differences. The two semi-permanent weather stations in the area (Campbell River airport and the Sentry Shoal weather buoy) were supplemented with 14 temporary weather stations maintained by the Institute of Ocean Sciences in support of aquaculture modelling (Figure 15). However, given the topography of the region, the data from point sources will under-represent the variability in the wind field between the weather stations. The most recent weather model developed by ECCC has a resolution of

250 m but even this is unable to provide accurate wind data for the narrow passages of the Discovery Islands (Foreman et al., 2012; Foreman et al., 2015b).

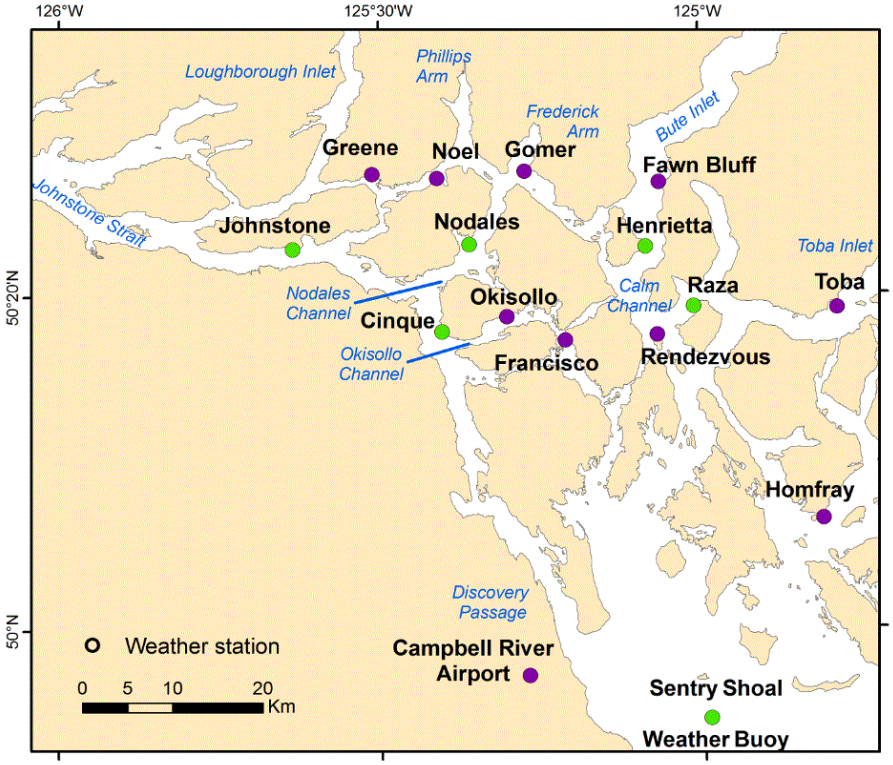

Figure 15. Weather station locations where wind speed and direction data were collected and analysed for the two year period 2010-2011. Wind roses from stations identified with green dots are given in Figure 16.

Wind data collected in 2010-2012 at 14 field weather stations, and two permanent stations (Campbell River airport and Sentry Shoal weather buoy) have been examined and reveal significant variability of wind conditions in the region. Figure 16 shows the variability in the wind field over this two year period as wind roses at six representative stations. The frequency of the wind blowing from a certain direction, and the strength of the winds from that direction, are seen to be influenced by topography, with the data from Sentry Shoal showing that it is the location least likely to be affected by local topographic influences. Data from stations such as Nodales, Henrietta, and Okisollo are clearly oriented along-channel, with stronger winds measured at Henrietta likely due to winds flowing out of Bute Inlet, or southerly winds from the Strait of Georgia.

Analysis of the hourly wind observations reveals that the strongest winds (greater than 10 m s^{-1}) are those most likely to influence the surface flows, and occur along Johnstone Strait and Discovery Passage and in the open waters of the northern Strait of Georgia. The dominant winds are from the northwest and southeast, in both strength and frequency of occurrence.

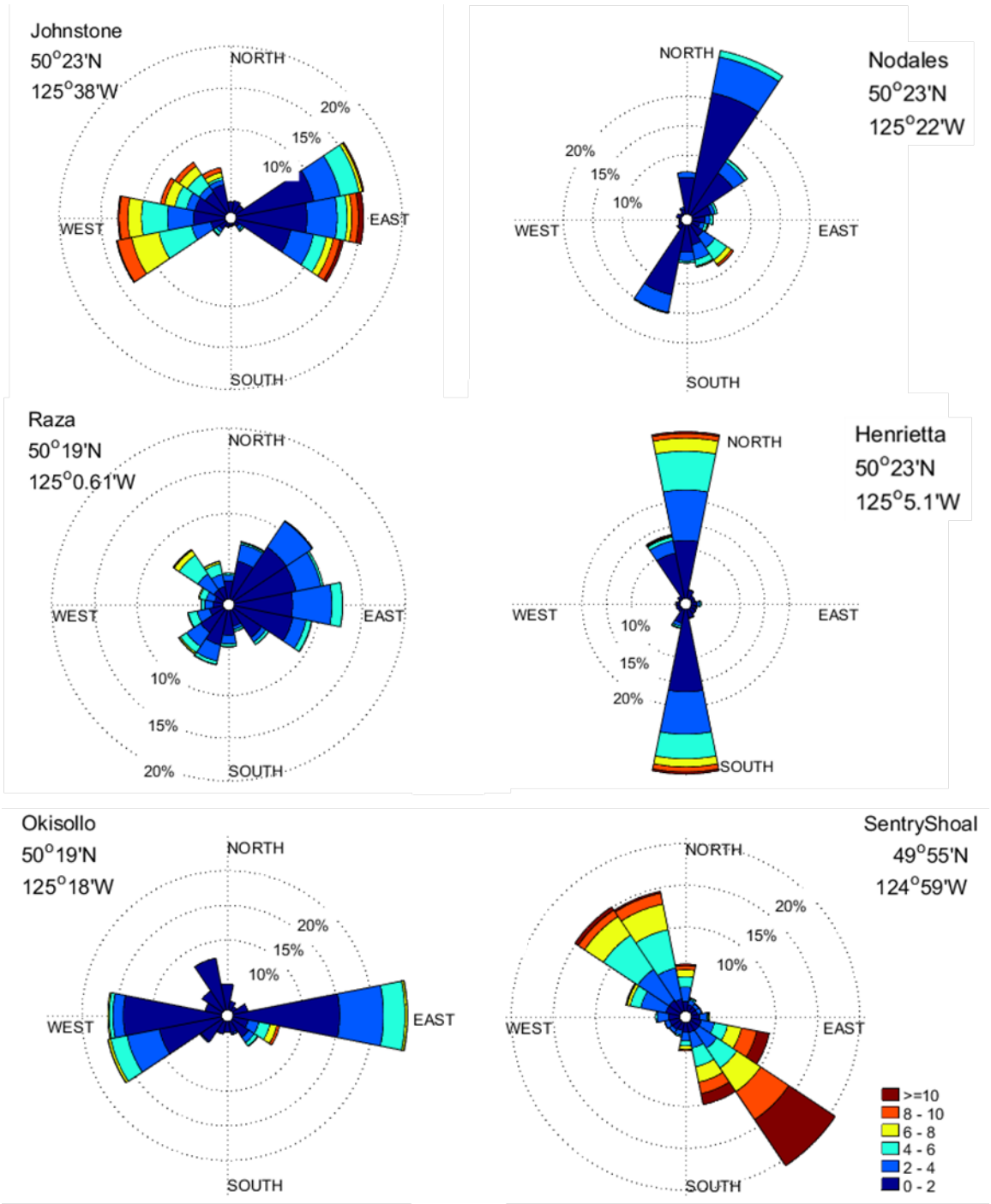

Figure 16. Wind roses, where wind speed is in units of m s^{-1} and wind direction is the direction from which the wind is blowing, computed from data collected in 2010 and 2011 at selected stations within the study area. Source: Sentry Shoal data from ECCC, other stations from temporary DFO weather station network.

SOLAR RADIATION AND ULTRAVIOLET LIGHT

Sunlight, and more specifically ultraviolet radiation (UV), is an important mechanism through which virus infectivity decays in seawater (Suttle and Chen, 1992; Garver et al., 2013). Several parameters related to sunlight influence the survival of bacteria and viruses in surface waters, including wavelength, depth, duration of exposure, turbidity and pathogen species (reviewed in Grant and Jones (2010)).

UV radiation is subdivided into UV-A (400-320 nm), UV-B (320-280 nm), and UV-C (280-200 nm) (Fleischmann, 1989). All solar UV wavelengths can damage the viral DNA or RNA but vary in efficiency depending on the wavelength (Rauth, 1965). While UV-B radiation is thought to be the primary component of sunlight inhibiting biological activities, longer wavelengths (UV-A) may also cause damage (Weinbauer et al., 1997). Although UV radiation can inactivate microorganisms in water, light dependent (photo-reactivation) and light-independent (dark repair) repair mechanisms can restore infectivity depending on the extent of damage (Weinbauer et al., 1997).

Sunlight or UV data specific to the Discovery Islands area is scarce. As part of the 2010-2011 field program solar radiation was measured at 14 weather stations using a Davis Instruments pyranometer that detects radiation at wavelengths of 300 to 1100 nanometers. Figure 17 displays these data from two locations and shows a similar seasonal pattern; more hours and higher levels of solar radiation during the summer. It is also evident that one station is exposed to sunlight from all directions during the day (Cinque), and the other (Henrietta) is in shadow during part of the day (from April to October). Given the steep topography of many of the fjords in the Discovery Islands region, the exposure of the water to radiation can vary significantly as these areas are blocked from direct sunlight.

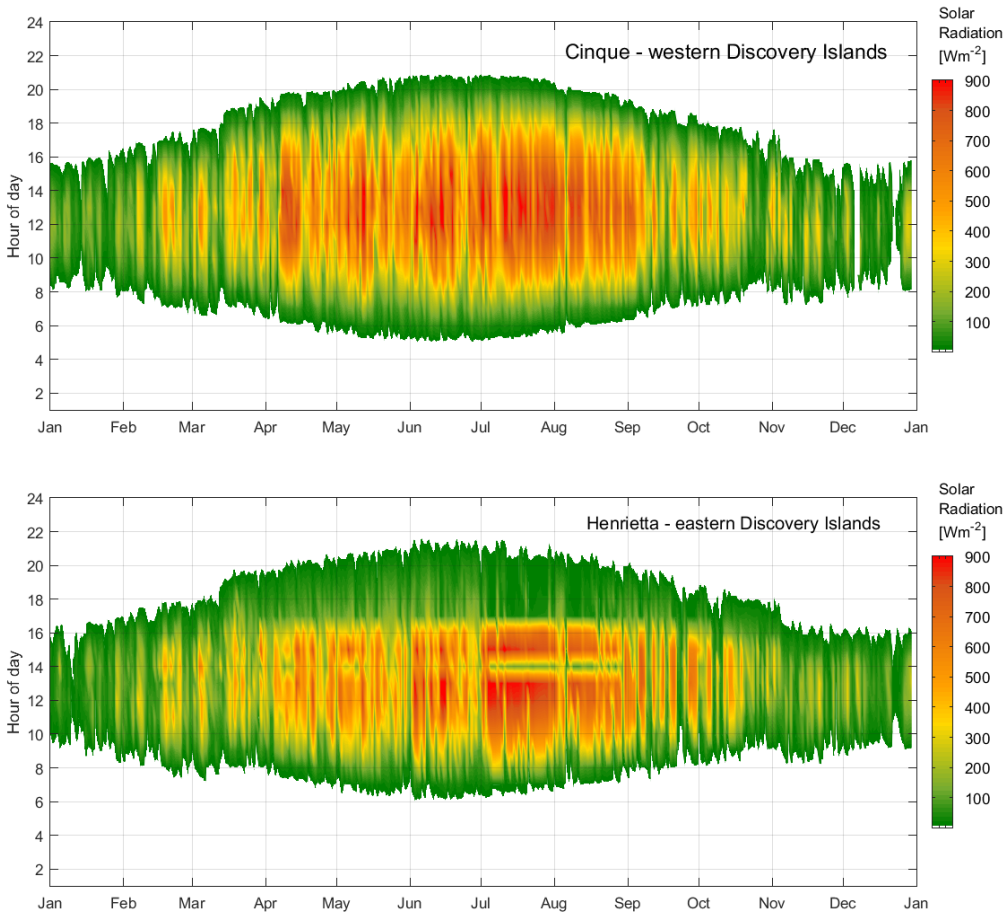

Figure 17. Solar radiation measured in 2010 and 2011 at Cinque and Henrietta in the Discovery Islands. Both panels show the seasonal and daily variation, and the events of high solar radiation (e.g., upper panel in mid-April). The lower panel shows how the shadow effect at specific times of the day (i.e., after 17h00) can reduce the incident solar radiation.

The annual cycle of solar radiation measured at Cinque (a station not affected by shading) is shown in Figure 18 and reveals the seasonal pattern. From April until August maximum solar radiation readings exceed 800 W m^{-2}, while from November through February they are typically below 400 W m^{-2}. In the winter months the average solar radiation levels are low due to a combination of reduced hours of daylight, and cloudy conditions.

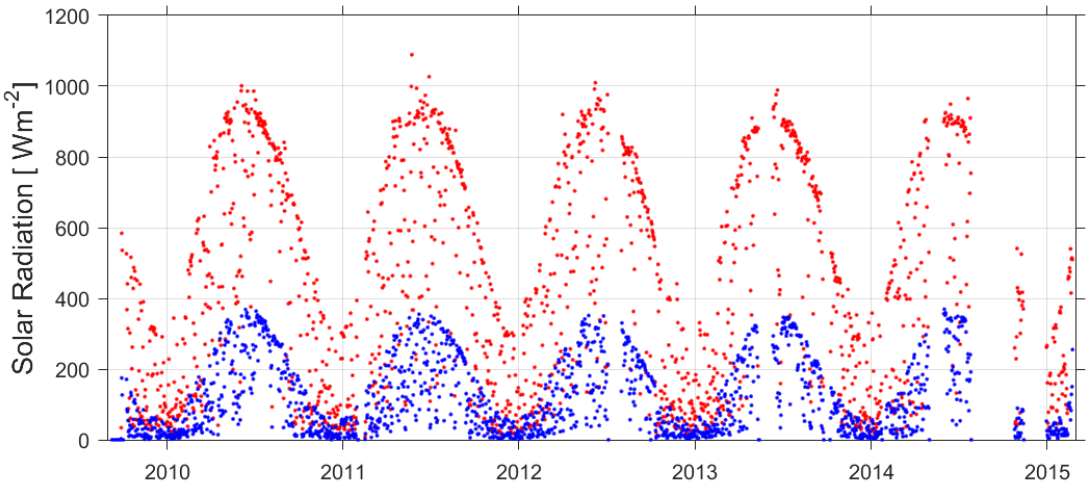

Figure 18. Solar radiation data from the Cinque weather station in the central Discovery Islands region. The red dots represent the maximum daily solar radiation observed and the blue dots show the solar radiation averaged over the day. Gaps in the record represent periods when the data did not pass the quality control standards.

The time series of sea surface UV radiation values, observed at the weather stations shown in Figure 15, for April and July 2010, are shown in Figure 19 and demonstrate the daily and seasonal difference in UV absorption ranging from 0 at night to maximum daily peak absorption between 5 to 35 W m^{-2} in April, and 24 to 54 W m^{-2} in July. Sunlight, cloud cover and solar angle contribute to the observed variations (Foreman et al., 2015b).

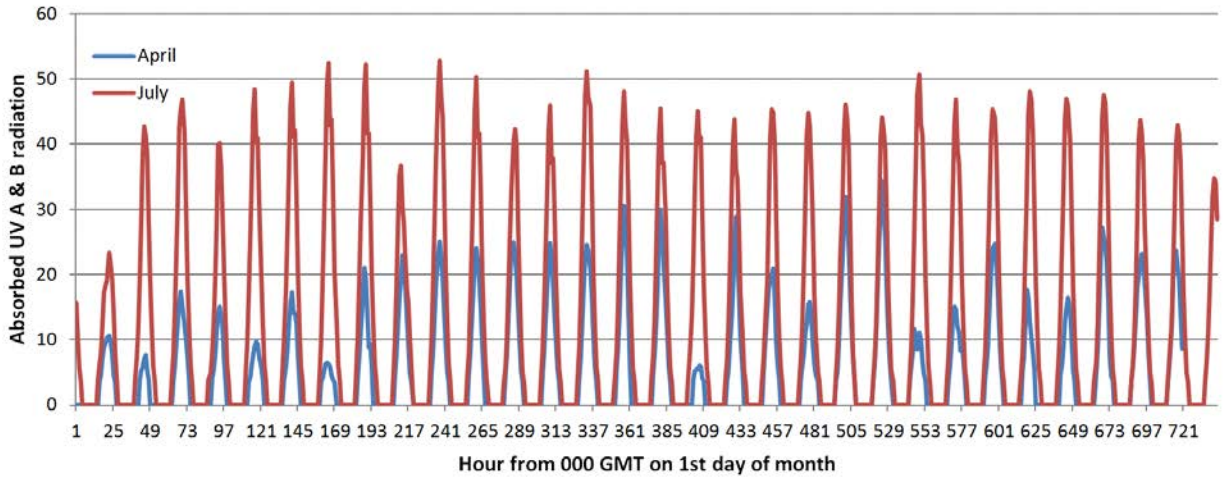

Figure 19. Average hourly UV (A and B) radiation (W m^{-2}) absorbed by the ocean in the Discovery Islands area for April and July 2010. Adapted from Foreman et al. (2015a).

UV reaching the earth's surface can penetrate seawater and damage the infectivity of bacteria and viruses in shallow waters (Sinton, 2006) by chemically modifying their genetic material (Lytle and Sagripanti, 2005). Damage to viral infectivity is proportional to the amount of radiation received (Regan et al., 1992; Suttle and Chen, 1992; Ronto et al., 1994; Garver et al., 2013) which decreases with depth in the marine environment (Fleischmann, 1989; Mann and Lazier,

1996) and is affected by water composition and dissolved organic matter (Diffey, 1991; Garver et al., 2013).

UV radiation is known to exponentially decay as it penetrates the upper surface of the ocean. Field measurements with a multichannel UV radiometer at two locations in the Discovery Islands in early September 2010 (Nodales Channel and at the entrance of Toba Inlet) provide the only depth profiles of UV extinction available. Figure 20 illustrates the exponential decay of the UV-A and UV-B measurements in Nodales Channel in September 2010, and also shows the fit of an exponential decay with a coefficient of -0.55 and -1.2 to the UV-A and UV-B data, respectively. It can be seen that pathogens at depths exceeding about 5 m are unlikely to be significantly affected by UV.

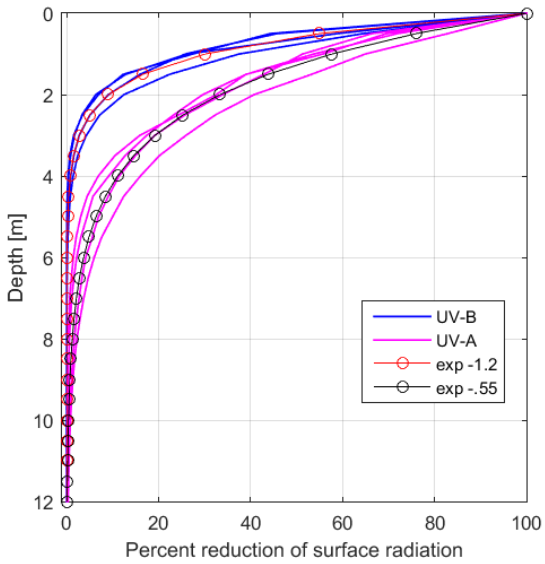

Figure 20. The attenuation of solar radiation with depth measured at Nodales Channel and at the entrance of Toba Inlet in the Discovery Islands in September 2010.

The impact that UV has on the deactivation of a pathogen will also depend on the length of time it is exposed. Solar radiation and UV attenuation information have been used to model the inactivation of a virus by calculating the absorption of UV radiation as a function of time, and applying a UV decay rate determined by fitting the data with an exponential curve. The 3D fields of density and currents from the hydrodynamic model determine the stratification and vertical mixing, and the time the pathogen is at a depth where UV inactivation can occur is determined by the particle tracking model. Although the UV data are sparse it is clear there is daily and seasonal variability, and the appropriate time and space scales important to this process continue to be evaluated.

BIOTA AND SUSPENDED SOLIDS

The extent to which biota and suspended solids influence the transmission and dispersal of pathogens in the water column is still an area of ongoing research. Evidence suggests that suspended biota in the water column accelerate the decay of infectivity of some viruses (Garver et al. (2013) and references therein) but suspended solids can also protect pathogens from UV light (Grant and Jones, 2010).

There are no directly-measured suspended biota or suspended solids data for the Discovery Islands area. However, light transmittance data, which can serve as a proxy for water clarity, were extracted from the MEDS databases based on observations between 1986 and 2015. These data demonstrate that light transmittance varies greatly over the year ranging from 0.2 to 63.6% (Figure 21). The highest ranges in light transmittance are observed in April and from June to September suggesting the highest variations in suspended biota and solids in the water column occur during these months. However, caution is required when interpreting these data given the gaps in time and in location. A DFO sampling program to collect suspended solids information is underway in the Strait of Georgia, with plans to expand it into the Discovery Islands.

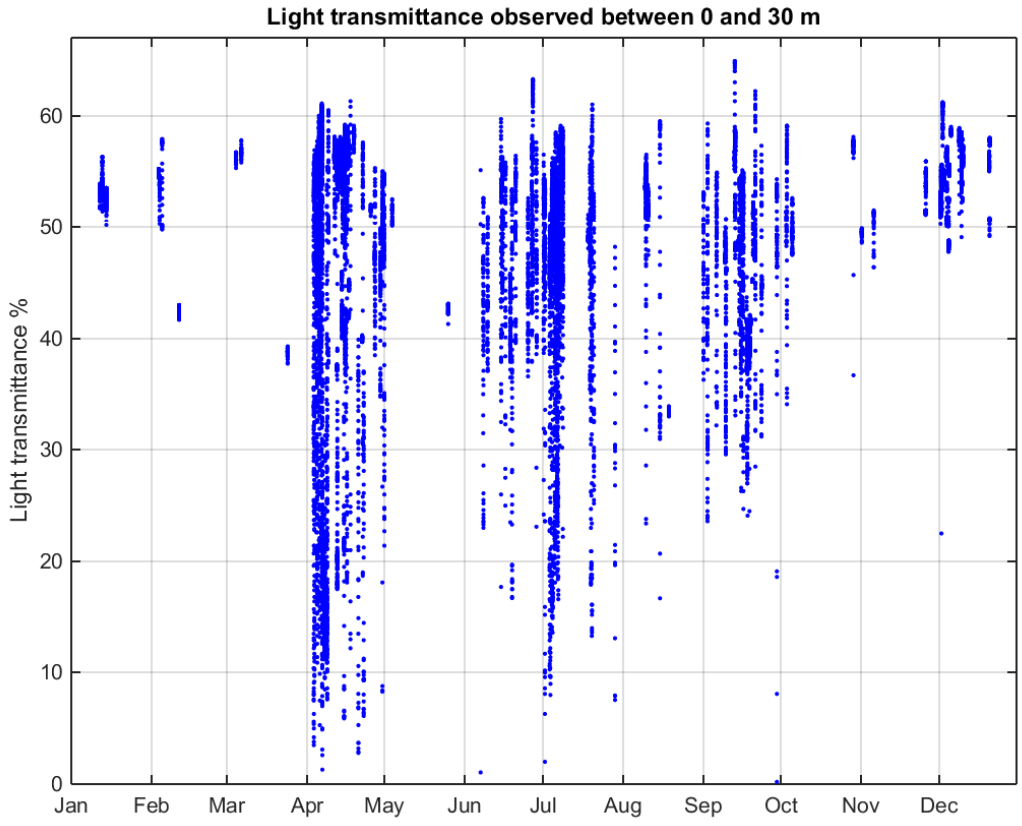

Figure 21. Percent light transmittance observed from the surface to the 30 meters depth in the Discovery Islands. Data were collected between 1986 and 2015 from various sources and extracted from the MEDS database.

MODELLING

HYDRODYNAMIC MODEL

The application of mathematical models to simulate the hydrodynamics in areas of aquaculture activity provides a better understanding of the physical oceanography that is relevant to pathogen risk management. The attributes of a hydrodynamic model suitable for this application include solving equations that conserve momentum and volume in three dimensions in order to characterize velocity and density variations arising from tidal, buoyancy and wind forcing. This is done by approximating the region of interest with an unstructured triangular grid capable of defining the fine scale details of the coastline and narrow passages and the use of sigma-

coordinate (terrain-following) depth layers to accommodate the significant variations in bottom depth. The model selected is the Finite Volume Community Ocean Model (FVCOM) (Chen et al., 2003; Chen et al., 2006; Chen et al., 2011) which has been reviewed and determined to provide a scientifically sound approach to represent the major circulation features in an area such as the Discovery Islands. See Foreman et al. (2015b) for further details on methods to evaluate model accuracy and a discussion of model limitations.

The generation of 3D velocity, temperature and salinity fields requires information to initialise the model, and field observations to validate the model output. During the simulation period wind, heat flux, tidal and buoyancy forcing must be specified. The three-dimensional temperature and salinity fields required as initial conditions were computed by interpolating and smoothing a combination of historical and recent CTD (conductivity, temperature, depth) observations; Figure 22 shows the surface salinity and temperature fields used to initialise the FVCOM model.

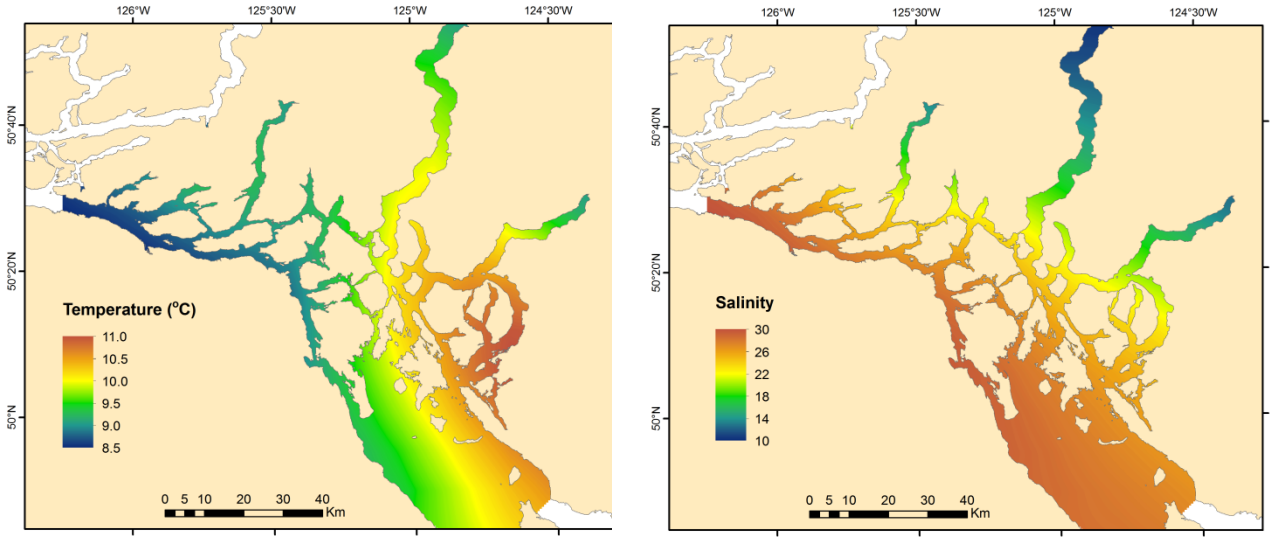

Figure 22. Surface salinity and temperature interpolated from climatology data (historical and recent) representing spatial variation for the month of April that was used to initialize the FVCOM model simulation described in Foreman et al. (2012). Adapted from Foreman et al. (2012).

FVCOM simulations for April and July 2010

The FVCOM hydrodynamic model was applied to simulate water flows in the Discovery Islands from April to October of 2010, and these flows can be used to track the dispersal of virus particles released at the locations of existing fish farms. The months of April and July are of particular interest as they reveal different environmental conditions during the out-migration period of juvenile salmon; specifically the surface outflow and lower salinity associated with snowmelt, and changes in solar radiation that significantly influence the fate of viruses.

Figure 23 shows the average near surface speeds for April and July 2010 generated by FVCOM. The tides are significant contributors to these fields, particularly in regions like southern Discovery Passage and Arran Rapids. When direct tidal contributions are removed from the monthly averages (right hand panels), differences between the April and July wind-driven and estuarine surface flows in locations like Calm and Sutil channels are more apparent. In particular, the July flows in those two channels are basically a continuation of surface estuarine flows emanating from Bute Inlet that in turn are largely caused by the Homathko River discharge. From April through July 2010, the Calm and Sutil estuarine flows gradually increase

in magnitude as the Homathko River discharge increases from about 100 to 800 $m^3 s^{-1}$. These flows then decrease in August and September but can rise again if there are heavy rainfall events. For example in 2010 a heavy rainfall in October increased the Homathko River discharge to over 1800 $m^3 s^{-1}$ (Figure 9 in Foreman et al. (2015a)).

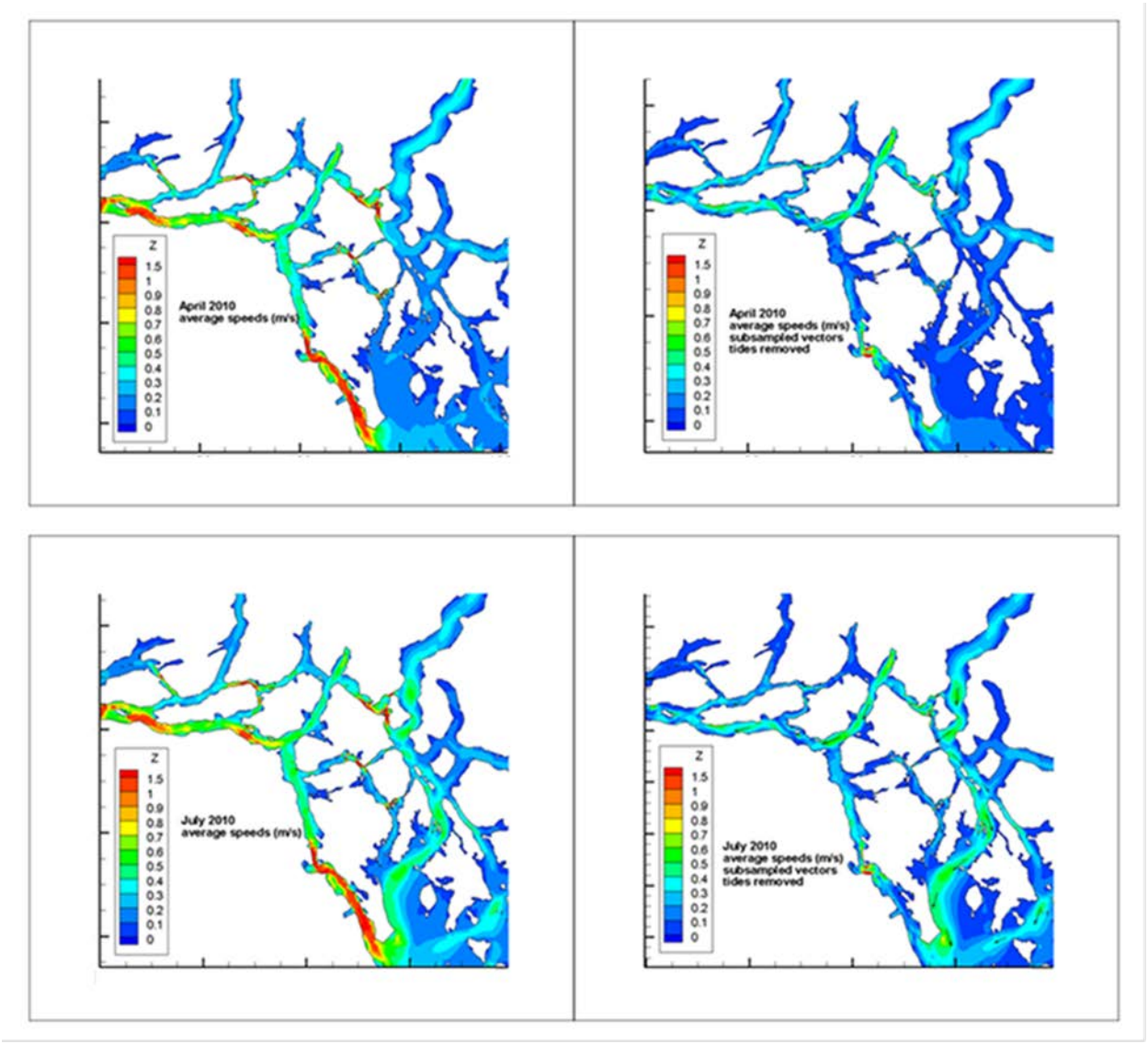

Figure 23. Average FVCOM current speeds at one meter depth for April and July 2010. Left panels include tides whereas right panels have the primary tidal contributions removed and include a few current vectors to show primary flow directions.

Comparison of ADCP observations and 2010 FVCOM simulations

In order to provide both a better understanding of the current patterns in the Discovery Islands and a partial evaluation of the ocean circulation and disease transmission models, nine acoustic Doppler current profiler (ADCP) moorings were deployed between 2009 and 2015 (Figure 13).

Near surface currents

Table 3 and Figure 24 compare monthly-averaged model currents for April and July 2010 with all observations made in April and July at the nine mooring sites. Note that these are revisions

of Table 1 and Figure 12 in Foreman et al. (2015a) that include more recent ADCP data from moorings HC11 and DS1 and a re-processing of all measurements so they have the same parameter settings. At some locations, this re-processing meant that more ADCP bins could be included in the near-surface averages. Model values are those for the grid element containing the ADCP location. As the observations spanned 2009 to 2015, some differences in the corresponding values can be attributed to inter-annual variability (e.g., note the differences in the HC11 and DS1 July 2014 and 2015 observed values).

The agreement of observed and model currents at sites DP1 and NC1 is very good, and is reasonable at the others, with the exception of DPN1. Differing directions in cases such as the April currents at OC1, CaC1, and DS1 are due to small scale eddies that have either not been accurately captured, or have been overly represented, by the model. As DPN1 is not near any of the salmon farms, inaccuracies in its mean model currents should not significantly affect the viral dispersion results. Nevertheless, the source of these inaccuracies suggest they arise from a combination of the three reasons described in Foreman et al. (2015a, pages 20-21).

Table 3. April and July monthly-averaged velocities (cm s^{-1}, degrees counter-clockwise from east) over the top 20 m (or portion thereof) at each of the ADCP locations (Figure 13). Column 6 shows observed root mean square speeds (cm s^{-1}) in the (u = east-west, v = north-south) directions after the tides and mean flow have been removed. Column 7 gives the average Homathko River discharge (m^3 s^{-1}) for the respective month.

1	2	3	4	5	6	7
Site	**Month and year**	**ADCP depth range (m) (and bin spacing)**	**Model average velocity for depth range or depth in column 3 (speed, dir.)**	**ADCP average velocity for depth range or depth in column 3 (speed, dir)**	**ADCP non-tidal RMS velocity for depth range or depth in column 3 (u,v)**	**Average Homathko River discharge**
DP1	April 2010 April 2011	6.6-21.6 (5.0) 6.4-21.4 (5.0)	7.9, 114	9.3, 130 7.3, 115	(9,9) (10,10)	91 94
DP1	July 2010	14.6-19.6 (5.0)	8.4, 117	11.0, 107	(14,16)	560
NC1	April 2010	6.3-21.3 (5.0)	5.0, 235	5.8, 238	(6,8)	91
NC1	July 2010	12.2-22.2 (5.0)	11.8, 237	8.2, 229	(4,4)	560
DPN1	April 2010	12.8-20.8 (8.0)	16.6, 183	13.1, 129	(18,16)	91
DPN1	July 2010	9.1-17.1 (8.0)	19.8, 190	5.3, 174	(16,13)	560
OC1	April 2011 April 2012	5.6-19.6 (2.0) 5.9-21.9 (4.0)	3.1, 112	5.3, 184 2.8, 166	(6,5) (6,5)	94 101
OC1	July 2011	5.9-21.9 (4.0)	8.1, 157	10.0, 184	(6,3)	674
CC1	April 2012	8.5-18.5 (5.0)	5.6, 229	8.6, 244	(7,7)	101
CC1	July 2011	8.5-18.5 (5.0)	6.4, 228	16.8, 209	(7,6)	674
SC1	April 2013	5.0-21.0 (2.0)	1.3, 43	2.0, 27	(5,9)	103
SC1	July 2012	6.0-22.0 (4.0)	6.8, 294	12.2, 298	(6,6)	680
CaC1	April 2013	5.9-21.9 (4.0)	16.3, 327	7.7, 16	(8,7)	103
CaC1	July 2012	5.9-21.9 (4.0)	38.3, 315	27.0, 330	(7,8)	680
HC11	April 2015	4.9-18.9 (2.0)	7.2, 265	5.0, 315	(3,8)	172
HC11	July 6-31, 2014 July 1-23, 2015	4.9-18.9 (2.0) 4.9-18.9 (2.0)	15.6, 280	10.7, 287 11.0, 286	(3,8) (3,8)	647 758
DS1	April 2015	4.0-20.0 (2.0)	3.1, 319	5.7, 256	(6,10)	172
DS1	July 6-31, 2014 July 1-22, 2015	4.0-20.0 (2.0) 44.0-20.0 (2.0)	23.1, 267	12.8, 251 11.3, 251	(6,13) (4,8)	647 758

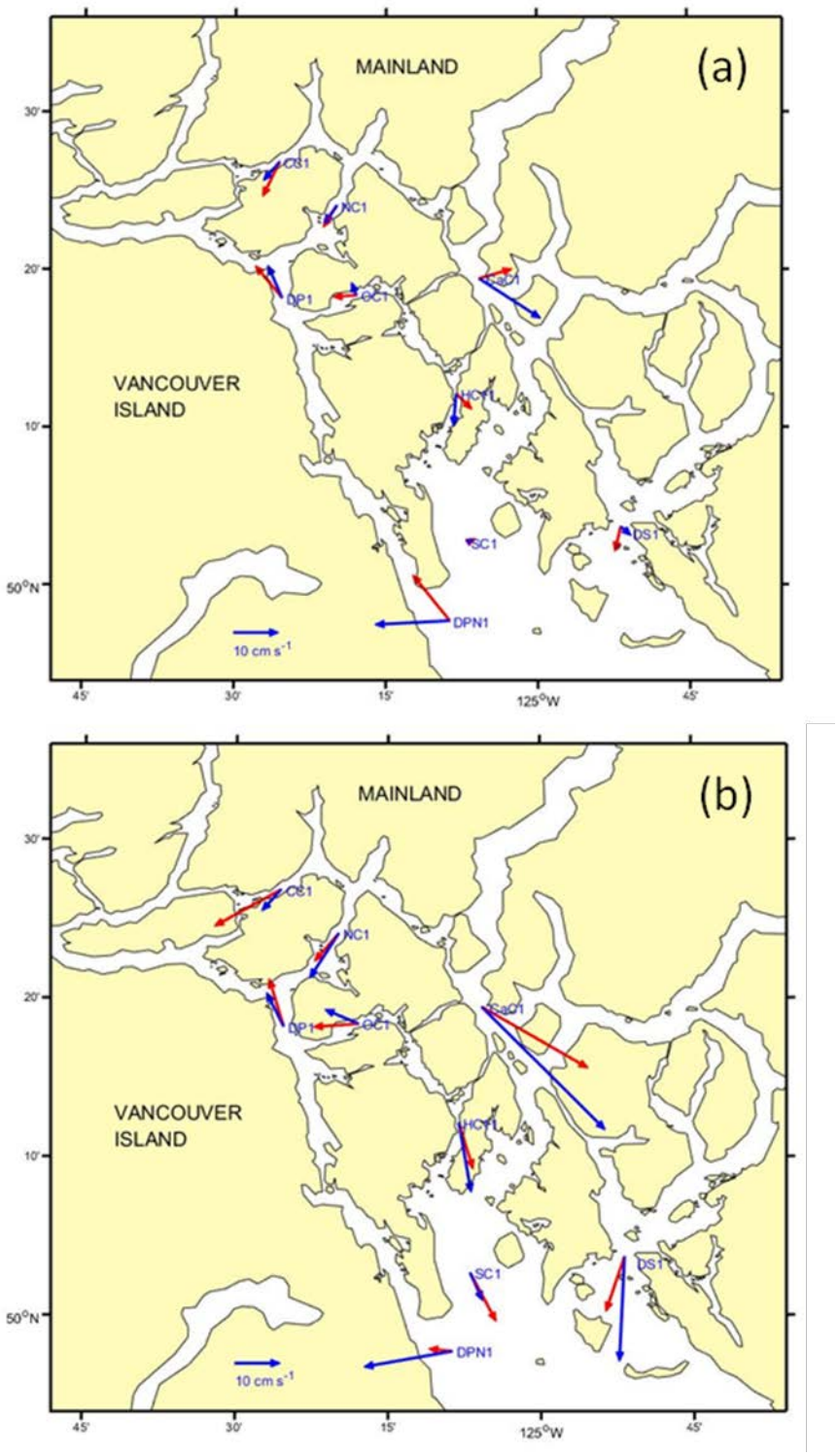

Figure 24. Monthly-averaged observed (red) and model (blue) near surface currents for April (a) and July (b), as listed and described in Table 3.

As given in Table 3 the average July currents are stronger than those in April by 30 – 100% (with the exception of DPN1). Though changes in wind direction may play a minor role, this increase is largely due to more freshwater discharge entering the system from the BC mainland

rivers. For example, differences between the April and July observed mean flows at moorings CaC1, SC1, HC11, and DS1 are largely a consequence of increased freshwater inputs to both Bute and Toba inlets. The model also shows an increase from April to July, although not necessarily in the same proportion as the observed currents. Some of this could be due to inaccurate forcing fields used by the model, namely:

i) Magnitudes of the river discharges (i.e., while the Homathko discharge was known, those from the Southgate, Toba and Brem (see Figure 3 in Foreman et al. (2012)) were estimated), and

ii) The zero salinities assigned to the river discharges which may contribute to the model salinity bias seen later in Table 6.

Other discrepancies could be due to inter-annual variability in the discharges. For example, column 7 in Table 3 shows that the average Homathko River discharge in July 2012 (when moorings CaC1 and SC1 were measuring) was 680 $m^3 s^{-1}$, about 20% larger than the 560 $m^3 s^{-1}$ average for July 2010 when the model was run. And in 2015, when the DS1 and HC11 moorings were in the water, the average July discharge was even larger at 758 $m^3 s^{-1}$. (Note: This simple comparison ignores the time lag it would take for the freshwater to move down Bute Inlet from the river mouth and eventually pass by these moorings.) Assuming a positive correlation between the strength of the Homathko River discharge and the surface estuarine flows at CaC1, SC1, DS1, and HC11, it is explained that the model simulation with the 2010 discharges would underestimate the near surface estuarine flows measured in 2012 and 2015. However that wasn't the case. So the too-large near-surface model flows must be due to another cause, most likely the low salinities indicated by Table 6. Further model runs are necessary to resolve this issue.

Column 6 in Table 3 gives the root mean square speeds (cm s^{-1}) in each the east-west and north-south directions after the mean flows (4^{th} column) and tides have been removed (all tidal analyses used exactly same tidal constituents and inference parameters.) They can be interpreted as a proxy for dispersion due to variations in the wind and freshwater discharge. Note that in most, but not all, locations they are larger in July than April.

Tidal currents

Similar comparisons were also carried out for the model and observed tidal currents. Table 4 shows tidal ellipse parameters (major semi-axis, angle of inclination, and phase lag) for the M2 and K1 constituents. As most of the ADCP locations are in narrow channels, the flows are basically rectilinear and the minor semi-axes are much smaller than the major semi-axes. So they have been ignored. Observed values are averaged over the same depth ranges given in column 3 of Table 3 while to facilitate computation and allow a single depth range for Figure 25, the model values were computed as averages over the range of 5-20 m.

Figure 25 superimposes the observed major semi-axis values on a contour plot of the model values, not only to provide an indication of agreement but also to demonstrate the high spatial variability within the Discovery region. In general, Table 4 indicates good agreement between the model and observed values. Some apparent large discrepancies, such as in the angle of inclination, θ, and phase lag, g, at OC1, arise from the specific definition of these variables. (θ is restricted to lie be between 0° and 180° while g is measured counter-clockwise from θ. So for M2 in April, θ = 170° is equivalent to θ = -10°. If this 180° shift is made to θ, the same must be done to g, changing 82° to 262°, and providing much better agreement.)

Table 4. Comparison of April and July M2 and K1 tidal ellipse parameters (major semi-axis (cm s^{-1}), angle of inclination (degrees counter-clockwise from east), and phase lag (degrees, UTC)) at the nine ADCP locations.

1	2	3	4	5	6
site	**Month, year**	**Model M2 ellipse parameters for 5-20 m depth range (speed, inclination, phase)**	**ADCP average M2 ellipse parameters for depth range or depth in column 3 of Table 1 (speed, inclination, phase)**	**Model K1 ellipse parameters for 5-20 m depth range (speed, inclination, phase)**	**ADCP average K1 ellipse parameters for depth range or depth in column 3 of Table 1 (speed, inclination, phase)**
DP1	April 2010 April 2011	57, 103, 106	49, 119, 109 40, 117, 106	12, 102, 332	10, 104, 336 7.5, 105, 346
DP1	July 2010	58, 105, 106	35, 123, 105	13, 111, 319	7.6, 110, 316
NC1	April 2010	19, 59, 256	8.2, 60, 265	5.1, 59, 136	3.0, 54, 167
NC1	July 2010	18, 57, 253	5.6, 49, 246	4.0, 57, 141	4.5, 49, 168
DPN1	April 2010	32, 165, 112	28, 151, 112	7.9, 159, 330	6.9, 123, 314
DPN1	July 2010	34, 170, 113	35, 164, 117	6.1, 144, 327	6.6, 162, 301
OC1	April 2011 April 2012	30, 15, 270	32, 170, 89 32, 173, 64	5.0, 17, 149	6.2, 167, 329 6.4, 173, 336
	July 2011	32, 10, 271	42, 180, 93	6.6, 7, 145	7.6, 174, 331
CC1	April 2012	39, 37, 263	37, 41, 233	7.7, 36, 124	7.7, 32, 111
CC1	July 2011	41, 37, 262	42, 37, 260	9.5, 36, 108	8.5, 42, 105
SC1	April 2013	4.3, 89, 329	3.9, 100, 328	3.1, 109, 233	4.3, 96, 225
SC1	July 2012	2.5, 63, 264	2.6, 93, 23	4.5, 101, 231	3.8, 128, 200
CaC1	April 2013	28, 129, 157	14,86,61	8.9, 142, 11	5.6,8,215
CaC1	July 2012	29, 123, 147	35, 130, 135	8.7, 135, 354	6.1, 123, 351
HC11	April 2015	27, 101, 98	32, 93, 125	5.1, 108, 315	5.7, 95, 345
HC11	July 6-31, 2014 July 1-23, 2015	28, 97, 94	42, 94, 128 36, 95, 132	5.8, 103, 329	7.8, 95, 331 5.9 ,96, 337
DS1	April 2015	9.6, 61, 349	6.1, 59, 7	6.0, 76, 265	5.3, 88, 251
DS1	July 6-31, 2014 July 1-22, 2015	9.7, 65, 354	3.9, 58, 2 5.0, 79, 10	5.5, 63, 210	8.2, 87, 254 7.0, 91, 254

It is noteworthy that both the model and observed ellipse parameters change from April to July (within the same year). This is primarily due to changes in stratification within the water column and thus changes in the baroclinic component of the tides. The barotropic component should remain relatively constant. At some locations, the M2 baroclinicity probably includes internal tides but further study would be needed to confirm this. Note that in all cases except SC1, the M2 model changes from April to July are smaller than those observed. This could be partially due to FVCOM deficiencies like the underlying hydrostatic assumption not being able to properly capture internal tides. But as with the mean velocity differences seen in Table 3, inter-annual variability between the 2010 model forcing conditions and those that were observed in other years might also account for some of the discrepancies. For example, HC11 and DS1 show clear differences in the ellipse parameters arising from analyses of their July 2014 and 2015 observations.

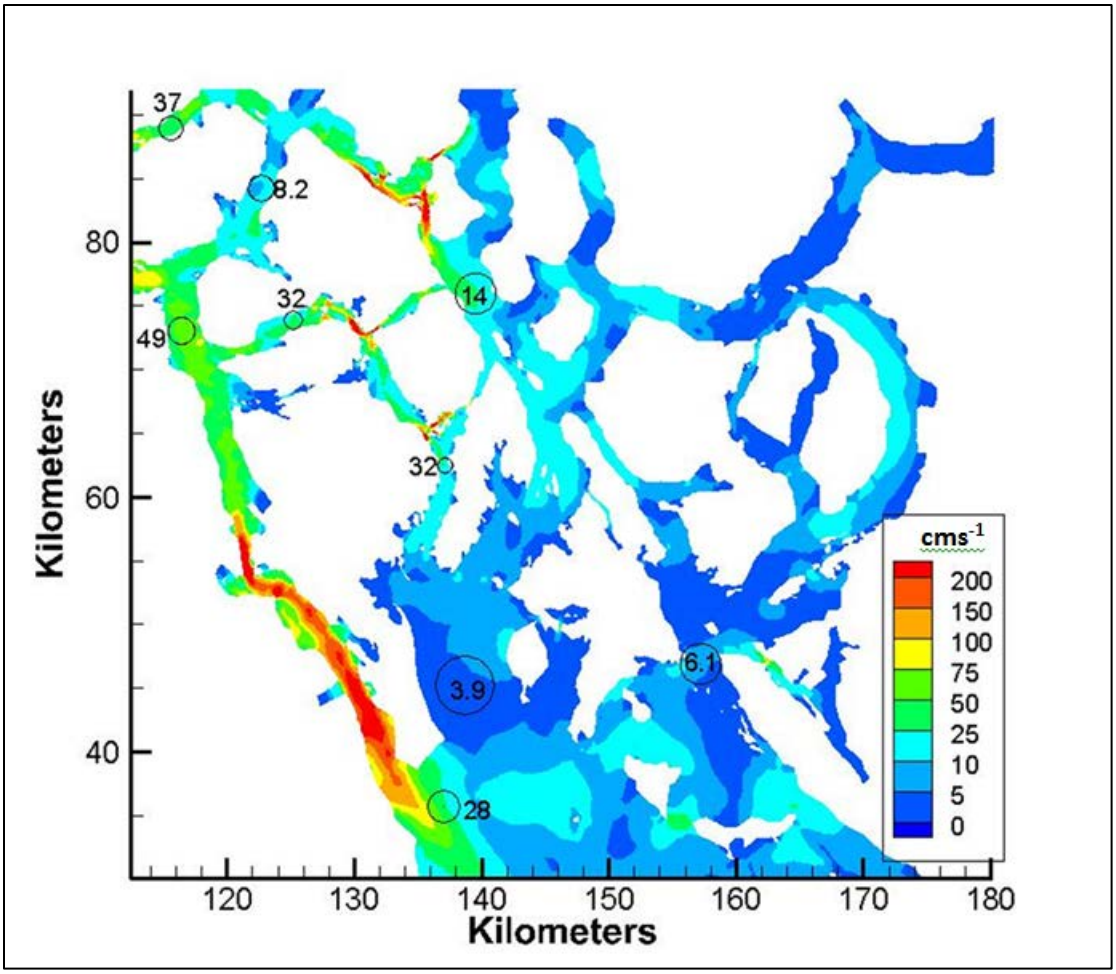

Figure 25. April monthly-averaged model (colour contours) and observed (black text beside or inside circle) M2 major semi-axis speeds (cm s^{-1}). Model values are averages between 5 and 20 m depth while observed values are averages over the depth ranges given column 3 of Table 3. Observed values are located at the center of the circles.

Comparison of farm observations and 2010 FVCOM simulations

Water quality information on Atlantic Salmon farms can further inform pathogen transfer environmental risk assessments. Table 5 presents the average monthly daily water quality observations collected between October 2005 and November 2015 on Atlantic Salmon farms located in the Discovery Islands. It should be noted that these data were provided without details about the quality control.

Table 5. Monthly average and standard deviations of daily water temperature, salinity and dissolved oxygen observations in near surface water (top 15 meters) on 16 Atlantic Salmon farms in the Discovery Islands from October 2005 to November 2015. n = the number of observations.

Month	Temperature (°C)		Salinity (ppt)		Dissolved oxygen (mmol m^{-3})	
	Mean ± std	n	Mean ± std	n	Mean ± std	n
January	7.7 ± 2.2	3781	29.4 ± 8.0	3331	311 ± 84	3255
February	7.7 ± 2.4	2811	29.7 ± 8.4	2380	328 ± 93	2321
March	7.6 ± 2.3	3066	29.8 ± 8.5	2654	341 ± 97	2578
April	8.2 ± 2.5	2925	29.9 ± 8.7	2665	348 ± 97	2311
May	9.3 ± 2.7	2739	29.8 ± 8.3	2507	353 ± 94	2144
June	10.5 ± 3.0	2508	29.3 ± 8.0	2298	329 ± 85	2014
July	11.5 ± 3.1	2005	28.9 ± 7.3	1740	311 ± 81	1787
August	11.5 ± 3.3	3570	29.1 ± 7.9	3310	281 ± 77	3310
September	11.0 ± 2.9	3202	29.1 ± 7.4	3008	262 ± 66	2942
October	10.2 ± 2.8	3677	28.9 ± 7.6	3446	261 ± 70	3452
November	8.9 ± 2.5	3725	29.0 ± 7.8	3460	271 ± 74	3497
December	8.2 ± 2.4	4064	29.5 ± 8.2	3539	300 ± 83	3436

Observations collected in near surface water (top 15 m) on Atlantic Salmon farms in the Discovery Islands show seasonal variations in surface water temperatures. Near surface waters are generally warmer in the summer, reaching maximum monthly average temperatures of 11.5°C in July and August (Table 5). They are coolest in the winter with minimum average monthly temperatures of 7.7°C in January and February. The average monthly salinities are seen to vary between 28.9 and 29.9 ppt in the top 15 m across the year with most of the variation occurring in the top five meters (Figure 8). Monthly averages for dissolved oxygen values vary between 261 and 353 mmol m^{-3}. Higher dissolved oxygen values are generally found near the surface all year around.

As the FVCOM model has only been run for April through October of 2010, a comparison could only be carried out for that time period and should provide a reasonable indication of model performance. Of course there will be inter-annual variability and with some effort to estimate the appropriate forcing fields, the model could be run for other years. But this has not been done due to resource constraints. The model was initiated with 2010 data representing the year with the best observational coverage to put the forcing fields together. Other years had many more gaps that would require considerable effort in filling.

Observed temperature and salinity data for 2005 to 2015 have been provided by the three Atlantic Salmon farm companies operating in the Discovery region: Marine Harvest Canada, Grieg Seafood, and Cermaq Canada. There are data from a total of 16 farms in 2010 but not all are available for each day or month. Since 2011 observations have been made daily. Although all farms measured values at five metres depth, only some have measurements at other depths such as 0 – 1 m. So for completeness, only the five meter values are compared here. Not all farms used the same equipment, thus the precision of their measurements may vary. In addition, the times at which observations were taken are not known. If they were, then the model could be sampled at those same times and potential biases (e.g., due to daily variations in temperature, as shown in the previous sub diurnal variations section) might be avoided. As it is, the model monthly averages were computed from all hourly values and average observed values were computed from all available daily values.

Table 6. Average absolute value of the differences between monthly averaged farm and model temperatures (°C) and salinities (ppt) at five meters depth.

Month (2010)	Number of farms	Average $\lvert T_{obs} - T_{mod} \rvert$ (ºC)	Average $\lvert S_{obs} - S_{mod} \rvert$
April	13	0.8	3.4
May	14	1.0	4.0
June	14	0.8	3.4
July	14	0.7	3.1
August	13	0.8	3.5
September	12	1.2	3.4
October	15	1.5	4.3

The monthly average temperature differences between farms are comparable (all within 1.5°C) and model parameter adjustments aimed at further improvements are probably not warranted at this time (Table 6). However, the salinity differences are much larger - consistently greater than three ppt; in almost all cases the model salinities were lower than the observed. As the initial model salinities on April 1 were computed from historical CTD observations and thereafter only changed in accordance with the model hydrodynamics (mainly advection and diffusion) and input from rivers, a consistently lower model bias suggests that either the prescribed salinities assigned to the freshwater discharges were too low, and/or the volume discharges were too large (i.e., too much freshwater entered the model domain).

As there were no direct measurements of salinity at the mouths of the rivers they were all prescribed zero salinity. Though this may be valid upstream from the mouth and beyond the extent of tidal mixing, it may not be the best value to choose right at the mouth. Rather, near surface values taken from CTD observations near the river mouths should perhaps have been chosen instead. In the absence of in-river observations, this is what was done with the river temperatures. In addition, there are uncertainties associated with some of the model freshwater volume discharges. Though daily discharges are available from Water Survey of Canada and BC Hydro for four rivers with the Discovery model domain, values for the other eight used in the model simulations were estimated based on sizes of their watersheds relative to those for which the discharges are known. Though reasonable, further observations are needed to assess the accuracy of this approach.

Representativeness of April and July 2010 conditions

The year 2010 was chosen for the simulation based on the availability of wind and river flow data to force the model, and solar radiation data to simulate the extent of virus decay. A comparison of conditions in 2010 with those observed in other years provides some measure of the applicability of the model results to years other than 2010.

The tidal flow in the model is based on astronomical forcing and bathymetry, neither of which will vary significantly from year to year. The winds, solar radiation, and fresh water flow vary seasonally and inter-annually, and how 2010 conditions compare to other years provides some measure of how representative the model results are of typical April and July conditions.

As shown in Figure 16 there are considerable differences in the wind speed and direction depending on the location in the Discovery Islands region. To compare the months of April and July in 2010 to other years, the data from the wind station at Sentry Shoal were chosen for their open exposure, and longer record of observations.

Figure 26 shows the wind observations made from the Sentry Shoal weather buoy in the northern Strait of Georgia. The left side of the figure refers to conditions in April, the right side to July conditions. The upper panel compares the daily wind vectors in 2010 (red) to those for the other years (blue). The middle and lower panels show the wind rose of hourly wind data from 2010, and all Aprils or Julys from 1993 to 2016, respectively. It can be seen that there were storm winds from the southeast for the first seven days of April 2010, but not atypical of storms seen in other years. The wind speeds for the remainder of April 2010 are considerably smaller, again consistent with other years. Wind conditions in July 2010 were less variable than those seen in other years, with the entire month dominated by winds from the north. Typical July conditions include a greater proportion of winds from the southeast.

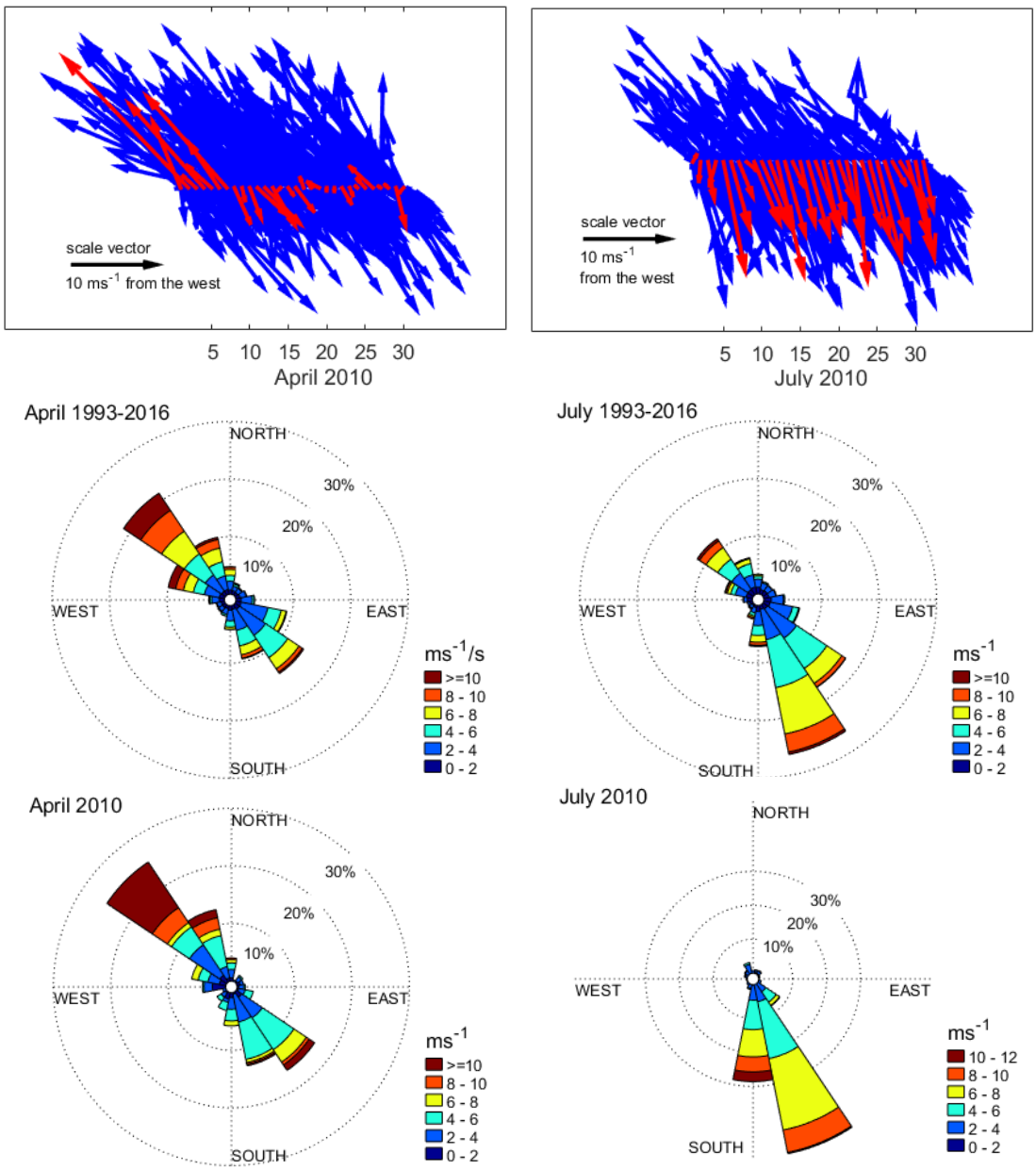

Figure 26. A comparison of wind data from the Sentry Shoal weather buoy in northern Strait of Georgia collected in April and July 2010, with observations made during the Aprils and Julys in the 24 other years from 1992 to 2016. The upper panels show the daily wind vectors in 2010 in red compared to all other years in blue. The wind roses show the distribution of wind speed and direction for all Aprils and Julys (middle panels) and for April and July 2010 only (lower panels). To correspond with the vector diagrams, the wind roses show wind direction as the direction towards which the wind is blowing. Source: ECCC.

Figure 27 compares the solar radiation observed at a DFO weather station in the central Discovery Islands region (Cinque Island, 50°18'N, 125°23'W) during April and July 2010, with data collected at the station between 2009 and 2015. While conditions in April are very close to the six year average, July 2010 experienced above average solar radiation exposure, but still within one standard deviation of data collected in the Julys between 2009 and 2015.

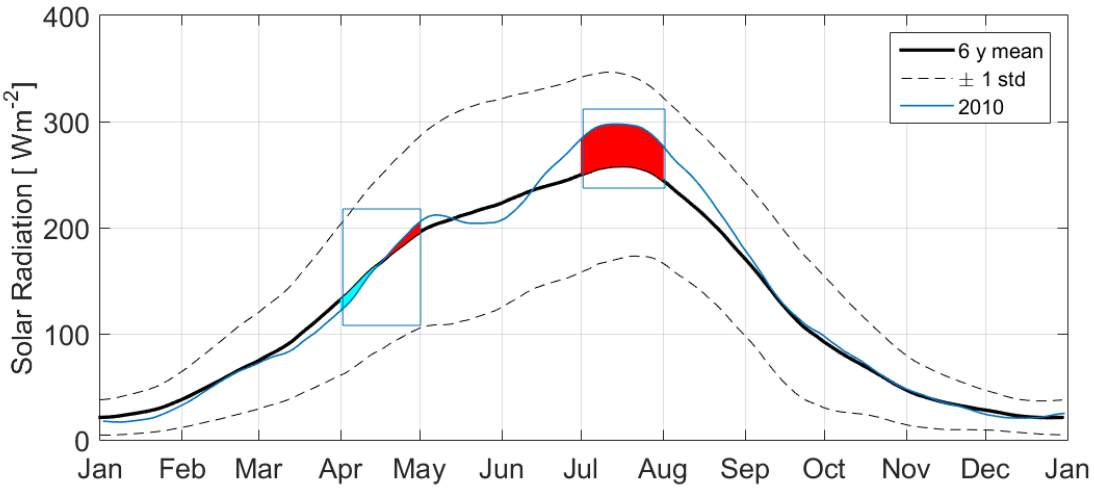

Figure 27. Solar radiation data from the Cinque Islands weather station in the central Discovery Islands region. The black solid line represents the mean daily solar radiation for each day of the year during the 2009-2015 period, the dashed lines represent one standard deviation of these daily values. The solid blue line is the corresponding solar radiation value for 2010, with April and July highlighted in red if the 2010 values exceed the mean, and blue if the 2010 values are below the mean. Source: DFO weather station network.

Figure 28 shows the water flow at the mouth of the Homathko River which represents a proxy for the forcing by freshwater on the circulation and salinity in the hydrodynamic model. The significance of the snowmelt in the river runoff from April to July is clear. During the two months of interest, April and July 2010, flows were below normal but within the variability expected during the 30 year record. Flows later in the year were abnormally low (September) and high (October).

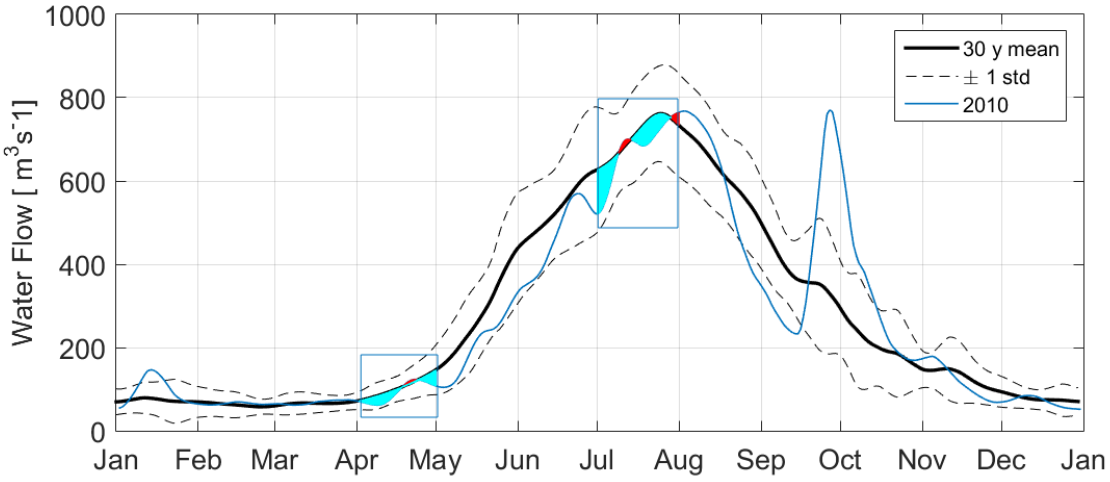

Figure 28. Water flow data from the mouth of the Homathko River in Bute Inlet. The black solid line represents the mean water flow for each day of the year during the 1982-2012 period, the dashed lines represent one standard deviation of these daily values. The solid blue line is the corresponding water flow value for 2010, with April and July highlighted in red if the 2010 values exceed the mean, and blue if the 2010 values are below the mean. (Source: Water Survey of Canada).

In summary, the wind and freshwater forcing conditions observed in April and July 2010 at the sites of comparison (Sentry Shoal – wind, Cinque – UV, Homathko River – fresh water) are not remarkably different from those observed during other years. Using these data with FVCOM can be expected to provide results that represent typical conditions.

PASSIVE PARTICLE TRACKING MODEL

In order to simulate the trajectories or dispersion of particles an offline Lagrangian particle tracking model developed at the Institute of Ocean Sciences was used. It inputs 3D velocity, temperature, and salinity fields computed and saved at hourly intervals by FVCOM to disperse and advect the particles. Pathogen inactivation can be determined by parameterizing the natural microbial community and using sea surface UV radiation data.

Pathogen tracking simulations can be modified to suit the issue of interest. Typically a cohort of particles is released at each farm location and tracked for a period of 10 days at 20 minute intervals. The number of particles per cohort can be adjusted but in general a cohort of 30 particles has been found to give a good balance between the representative diffusion characteristics of the cohort and the computer resources required to run the model. The particles are initially distributed over a volume of water representative of a typical fish farm (100 m by 100 m by 20 m). The model calculates the inactivation of the particle relative to its initial concentration and as such, the results can be scaled to reflect different shedding rates.

Figure 29 illustrates the dispersion clouds resulting from a simulation conducted under April 2010 conditions in which passive particles were released at the surface from 32 farms located in the Discovery Islands and tracked for ten days. As expected, based on the predominant northwestward surface estuarine flow in the area, the simulation indicated that particles could reach Johnstone Strait within 2.5 days (Foreman et al., 2015b). The simulation also indicated that a small percentage of particles travelled southeastward and reached the Strait of Georgia (40 km away) within five days.

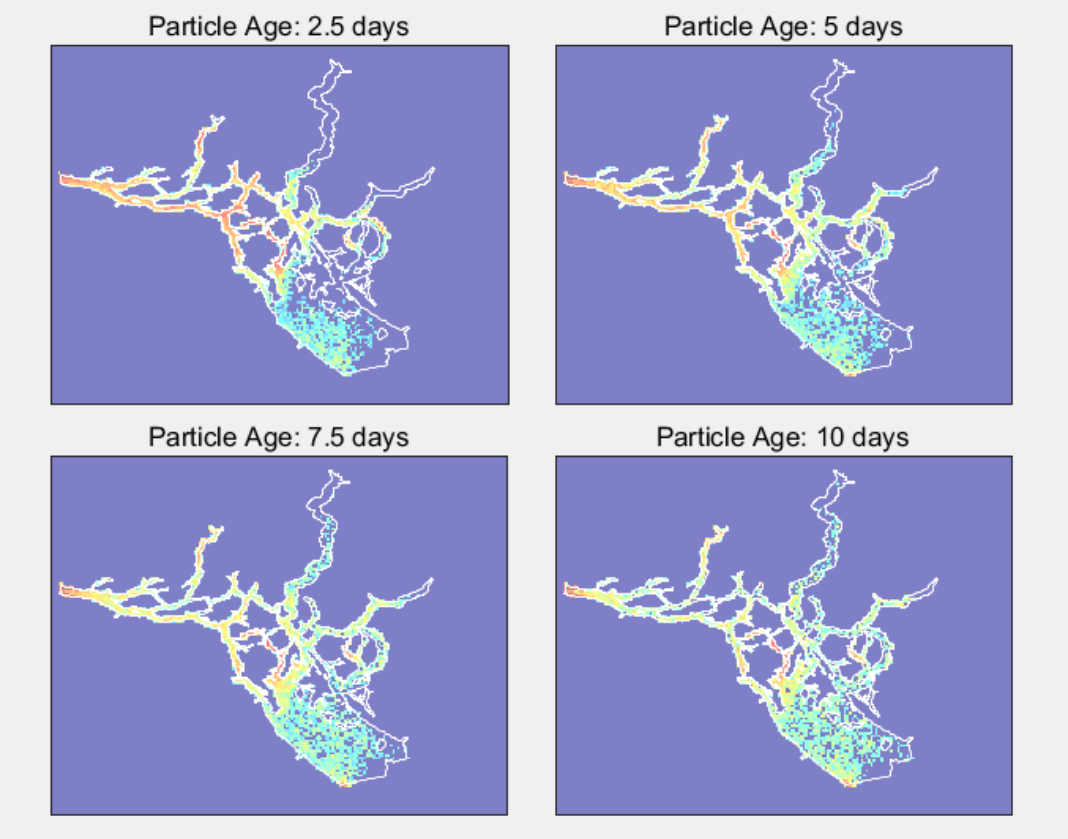

Figure 29. Dispersion clouds arising after 2.5, 5, 7.5, and 10 days from hourly passive particle releases over the month of April, 2010 at 32 farms within the Discovery Islands area. Red and turquoise colours, respectively, denote higher and lower concentrations. Adapted from Foreman et al. (2015a).

Passive particle dispersion is also expected to vary seasonally. Additional simulations showed that particles could travel 10% further and disperse 31% more widely in July compared to April 2010 when released from the same locations (Foreman et al., 2015a).

The scope and accuracy of the above simulation is an important consideration for environmental risk assessments. When the simulated dispersal predictions were compared to actual trajectories of GPS tracked drifters released in Knight Inlet, north of the Discovery Islands, the observed trajectories were similar in direction but the actual drifters traveled less distance than the corresponding modelled particles in the first six hours after release (Foreman et al., 2015b). However, this initial inconsistency was not observed 24 hours after release suggesting that the passive particle tracking model provided realistic simulations of expected trajectories and traveled distances. Though some GPS drifter studies have also been carried out in the Discovery Island region, and more are planned, the results have yet to undergo a detailed analysis and comparison with analogous model simulations.

Another limitation of the passive particle dispersion model is the timing and duration of the simulation. The initial dispersion of modelled particles was only carried out for April 2010 and subsequently has only been extended to July 2010 (Foreman et al., 2015a). The use of those results to inform pathogen transfer environmental risk assessments should be considered within the scope of those studies and caution is therefore advised in extrapolating outside those specific time periods.

Non-passive particle tracking models have also been developed to simulate dispersal of specific biological entities such as sea lice (Stucchi et al., 2011; Foreman et al., 2015b) and pathogens (Foreman et al., 2015a; Foreman et al., 2015b).

RECOMMENDATIONS

The foregoing analyses of environmental data and model output only summarize what has been done to date. Clearly further work could be carried out to fill in observational gaps and to improve both the credibility and temporal coverage of the model. The following list is in no particular order.

- More work needs to be done to reduce discrepancies between observed and model salinities at the farms. Most of the discrepancies are likely due to poorly chosen river salinities, and these could be improved with further sensitivity studies and, resources permitting, observations near river mouths.
- If farm data are to be used for oceanographic purposes, work should also be carried out to assess, standardize, and possibly improve, the accuracy of temperature, salinity and oxygen observations taken at the farms. This would have to be done in collaboration with industry.
- The GPS drifter studies carried out in the Discovery Island region should be analysed in more detail and compared with analogous model simulations.
- In order to further evaluate the accuracy of model near surface temperatures, they should be compared to LANDSAT (or other satellite) images.
- As validation of the models has been carried out for April and July 2010 only, the circulation and particle tracking models should be run for other years and months.
- More field work should be carried out to investigate spatial and temporal variations in UV penetration into the water column, with particular attention to the roles of biota and suspended solids.

CONCLUSIONS

The Discovery Islands area is a complex network of islands, narrow channels and deep fjords with significant seasonal and spatial variations in oceanographic profiles. Current knowledge about the ocean circulation in the Discovery Islands is mainly derived from model simulations from April to October 2010 and ADCP moorings deployed over 2009-2015. The key findings, and their related uncertainties, to inform pathogen transfer environmental risk assessments in the area are summarized below.

- The physical oceanography of the Discovery Islands is characterized by strong tidal currents, significant freshwater flow due to river runoff and snowmelt, and surface currents driven by winds that vary in speed and direction due to the steep topography typical of fjord regions.
- Oceanographic conditions in the Discovery Islands region vary both seasonally and regionally, with a monthly average temperature range of 6 to 14^{0}C (measured minimum and maximum of 3 and 24^{0}C), monthly average salinity range between 23 and 31 (measured minimum and maximum of close to 0 and 32) and monthly average levels of dissolved oxygen ranging between 170 and 340 mmol m^{-3} (measured minimum and maximum of 50

and 550 mmol m^{-3}). Waters in the central Discovery Islands (in the vicinity of the fish farms) are generally well-mixed.

- UV is observed to vary seasonally with summer solar radiation often exceeding 800 W m^{-2}, and is reduced during periods of cloudiness and at night. Measurements show that as UV penetrates the water it is reduced exponentially to less than one percent of its surface value within 10 m.
- Tidal currents of at least 1 m s^{-1} are common and in some areas can transport water over 14 km in one direction until the tide changes.
- River discharges throughout the region force surface currents that generally flow seaward.
- Wind can drive surface currents on seasonal and shorter time scales.
- A Discovery-region hydrodynamic model (FVCOM) has been developed to simulate the circulation due to the forcing fields described above.
- A coupled particle tracking model has also been developed to simulate the dispersal of particles. The dispersion time and spatial scales vary depending on the tides, river discharges and winds.
- As wind and freshwater forcing conditions observed in April and July 2010 were not remarkably different from those observed during other years, the circulation and particle tracking model results for those time periods should be considered representative of any April and July.

REFERENCES CITED

Chen, C., Beardsley, R. C., Cowles, G., Qi, J., Lai, Z., Gao, G., Stuebe, D., Xu, Q., Xue, P., Ge, J., Ji, R., Hu, S., Tian, R., Huang, H., Wu, L. and Lin, H. 2011. An Unstructured Grid, Finite-Volume Coastal Ocean Model. FVCOM User Manual. 3rd ed. Massachusetts Institute of Technology, Cambridge, Massachusetts 02139. 315 p.

Chen, C., Beardsley, R. C. and Cowles, G. W. 2006. An unstructured-grid, finite-volume coastal ocean model (FVCOM) system. Oceanogr. 19(1): 78-89.

Chen, C., Liu, H. and Beardsley, R. C. 2003. An unstructured grid, finite-volume, three-dimensional, primitive equations ocean model: application to coastal ocean and estuaries. K. Atmos. Ocean. Technol. 20: 159-186.

Cohen, B. I. 2012. Recommendations, summary, process. The Uncertain Future of Fraser River Sockeye. Vol. 3. Minister of Public Works and Government Services Canada, Publishing and Depository Services, Public Works and Government Services Canada, Ottawa, ON K1A 0S5. 211 p.

DFO. 2015. Marine Finfish Aquaculture Licence under the Fisheries Act. Aquaculture Management Division.

Diffey, B. L. 1991. Solar ultraviolet radiation effects on biological systems. Rev. Phys. Med. Biol. 36(3): 299-328.

Fleischmann, E. M. 1989. The measurement and penetration of ultraviolet-radiation into tropical marine water. Limnol. Oceanogr. 34(8): 1623-1629.

Foreman, M., Guo, M., Garver, K. A., Stucchi, D., Chandler, P., Wan, D., Morrison, J. and Tuele, D. 2015a. Modelling infectious hematopoietic necrosis virus dispersion from marine salmon farms in the Discovery Islands, British Columbia, Canada. PLoS One 10(6): e0130951.

Foreman, M. G. G., Chandler, P. C., Stucchi, D. J., Garver, K. A., Guo, M., Morrison, J. and Tuele, D. 2015b. The ability of hydrodynamic models to inform decisions on the siting and management of aquaculture facilities in British Columbia. DFO Can. Sci. Advis. Sec. Res. Doc. 2015/005. vii + 49 p.

Foreman, M. G. G., Stucchi, D. J., Garver, K. A., Tuele, D., Isaac, J., Grime, T., Guo, M. and Morrison, J. 2012. A circulation model for the Discovery Islands, British Columbia. Atmos. Ocean. 50(3): 301-316.

Garver, K. A., Mahony, A. A. M., Stucchi, D., Richard, J., Van Woensel, C. and Foreman, M. 2013. Estimation of parameters influencing waterborne transmission of infectious hematopoietic necrosis virus (IHNV) in Atlantic salmon (*Salmo salar*). PLoS One 8(12): e82296.

Grant, A. A. M. and Jones, S. R. M. 2010. Pathways of effects between wild and farmed finfish and shellfish in Canada: potential factors and interactions impacting the bi-directional transmission of pathogens. DFO Can. Sci. Advis. Sec. Res. Doc. 2010/018. vi + 58 p.

Lewis, E. L. and Perkin, R. G. 1981. Practical salinity scale 1978: conversion of existing data. Deep-Sea Res. 28A(4): 307-328.

Lim, J., Brown, L. and Ersahin, K. 2015. LANDSAT sea surface termperature maps for the Broughton Archipelago and Discovery Islands, BC. ASL Environmental Sciences. PR-889. 44 p.

Lin, Y., Jiang, J., Fissel, D. B., Foreman, M. G. and Willis, P. G. 2011. Application of finite-volume coastal ocean model in studying strong tidal currents in Discovery Passage, British Columbia, Canada. Estuar. Coast. Model. 1: 99-117.

Lytle, C. D. and Sagripanti, J.-L. 2005. Predicted inactivation of viruses of relevance to biodefense by solar radiation. J. Virol. 79(22): 14244-14252.

Mann, K. H. and Lazier, J. R. N. 1996. Dynamics of marine ecosystems: biological-physical interactions in the oceans. 3rd ed. John Wiley & Sons Ltd. 394 p.

Rauth, A. M. 1965. Physical state of viral nucleic acid and sensitivity of viruses to ultraviolet light. Biophys. J. 5(3): 257-273.

Regan, J. D., Carrier, W. L., Gucinski, H., Olla, B. L., Yoshida, H., Fujimura, R. K. and Wicklund, R. I. 1992. DNA as a solar dosimeter in the ocean. Photochem. Photobiol. 56(1): 35-42.

Ronto, G., Gaspar, S., Grof, P., Berces, A. and Gugolya, Z. 1994. Ultraviolet dosimetry in outdoor measurements based on bacteriophage-T7 as a biosensor. Photochem. Photobiol. 59(2): 209-214.

Sinton, L. W. 2006. Biotic and abitoic effects. *In* Oceans and Health: Pathogens in the Marine Environment. Belkin, S. and Colwell, R. R. (eds.). Spinger Science, New York, USA. pp 69-92.

Stucchi, D. J., Gao, M., Foreman, M. G. G., Czajko, P., Galbraith, M., Mackas, D. L. and Gillibrand, P. A. 2011. Modeling sea lice production and concentrations in the Broughton Archipelago, British Columbia. *In* Salmon Lice: An Integrated Approach to Understanding Parasite Abundance and Distribution. Jones, S. R. M. and Beamish, R. J. (eds.). Wiley-Blackwell, Oxford, UK. pp 117-150.

Suttle, C. A. and Chen, F. 1992. Mechanisms and rates of decay of marine viruses in seawater. Appl. Environ. Microbiol. 58(11): 3721-3729.

Thomson, R. E. 1981. Oceanography of the British Columbia coast. Can. Spec. Publ. Fish. Aquat. Sci. 56: 291 p.

Tinis, S. W. and Thomson, R. E. 2004. Operational modelling of southwest British Columbia waters using the Princeton Ocean model. Institute of Ocean Sciences. Unpublished Works.

Weinbauer, M. G., Wilhelm, S. W., Suttle, C. A. and Garza, D. R. 1997. Photoreactivation compensates for UV damage and restores infectivity to natural marine virus communities. Appl. Environ. Microb. 63(6): 2200-2205.

APPENDIX A: TEMPERATURE, SALINITY AND OXYGEN DATA

Table 7. Monthly average water temperature (0 to 30 m) across nine regions in the Discovery Islands (1932 to 2015). N/A: not applicable: no data.

Month	Descriptive statistics	Bute Inlet	Eastern channels	Johnstone Strait and Discovery Passage	Loughborough Inlet	Northern Strait of Georgia	Northwestern channels	Phillips Arm, Frederic Arm and Cordero Channel	Ramsay Arm and Toba Inlet	Western channels
January	**mean ± std**	**6.0 ± 1.3**	**7.1 ± 0.9**	**7.7 ± 0.47**	**N/A**	**7.5 ± 1.0**	**N/A**	**N/A**	**N/A**	**N/A**
	range	2.3 to 7.9	5.7 to 8.3	6.9 to 8.3	N/A	3.3 to 8.6	N/A	N/A	N/A	N/A
	n = prof (obs)	5 (40)	28 (31)	29 (355)	N/A	29 (619)	N/A	N/A	N/A	N/A
February	**mean ± std**	**7.0 ± 0.8**	**7.1 ± 0.6**	**7.6 ± 0.2**	**6.5 ± 1.0**	**7.4 ± 0.7**	**7.7 ± 0.2**	**N/A**	**6.8 ± 0.9**	**N/A**
	range	3.3 to 8.2	4.5 to 8.4	6.5 to 7.8	5.0 to 7.0	5.4 to 8.7	7.2 to 7.9	N/A	3.7 to 7.9	N/A
	n = prof (obs)	30 (290)	30 (274)	26 (304)	4 (4)	29 (1290)	30 (30)	N/A	7 (22)	N/A
March	**mean ± std**	**7.1 ± 0.6**	**7.4 ± 0.3**	**7.7 ± 0.3**	**N/A**	**7.8 ± 0.6**	**N/A**	**7.7 ± 0.1**	**7.5 ± 0.6**	**7.7 ± 0.1**
	range	3.8 to 8.5	6.6 to 8.3	6.8 to 8.8	N/A	5.3 to 9.5	N/A	7.1 to 7.9	6.9 to 10.6	7.5 to 7.9
	n = prof (obs)	8 (147)	30 (437)	29 (1221)	N/A	31 (1042)	N/A	30 (433)	9 (41)	30 (710)
April	**mean ± std**	**8.5 ± 0.6**	**8.2 ± 0.5**	**7.9 ± 0.7**	**8.8 ± 0.7**	**8.8 ± 0.7**	**8.1 ± 0.0**	**8.4 ± 0.3**	**8.5 ± 0.1**	**8.1 ± 0.2**
	range	7.8 to 10.2	7.0 to 11.3	7.0 to 9.5	8.3 to 10.6	7.0 to 13.8	8.1 to 8.1	7.9 to 9.3	8.4 to 8.6	7.8 to 9.3
	n = prof (obs)	30 (98)	30 (2186)	56 (1589)	27 (27)	30 (4757)	29 (29)	30 (340)	25 (25)	30 (802)
May	**mean ± std**	**9.4 ± 1.7**	**10.9 ± 1.9**	**8.7 ± 0.4**	**8.2 ± 0.9**	**10.8 ± 1.63**	**9.4 ± 0.9**	**8.9 ± 0.6**	**9.7 ± 1.8**	**10.1 ± 0.8**
	range	5.9 to 16.7	6.9 to 18.3	7.6 to 10.9	5.5 to 10.6	7.6 to 15.5	7.8 to 10.9	8.3 to 12.3	6.9 to 13.9	8.6 to 11.5
	n = prof (obs)	30 (1204)	29 (172)	30 (3600)	5 (29)	29 (569)	30 (92)	28 (153)	29 (85)	30 (191)
June	**mean ± std**	**10.6 ± 2.0**	**12.3 ± 2.8**	**10.2 ± 1.3**	**10.4 ± 2.4**	**12.5 ± 2.4**	**10.4 ± 0.2**	**10.0 ± 0.5**	**12.9 ± 2.1**	**11.0 ± 0.6**
	range	6.7 to 19.3	8.1 to 19.2	8.4 to 18.4	8.1 to 17.1	8.1 to 19.4	9.4 to 11.5	9.6 to 13.5	8.3 to 17.2	9.1 to 11.9
	n = prof (obs)	30 (659)	30 (486)	31 (1217)	29 (75)	30 (3574)	31 (94)	30 (190)	30 (164)	30 (353)
July	**mean ± std**	**10.7 ± 1.5**	**13.9 ± 2.3**	**10.5 ± 1.0**	**10.8 ± 2.1**	**12.2 ± 2.6**	**N/A**	**10.5 ± 0.9**	**11.9 ± 2.3**	**11.1 ± 0.6**
	range	7.8 to 15.8	8.5 to 22.6	9.1 to 15.8	8.3 to 17.9	7.5 to 20.5	N/A	10.0 to 16.6	9.1 to 17.2	9.9 to 12.2
	n = prof (obs)	29 (731)	28 (2164)	30 (901)	7 (130)	30 (3517)	N/A	28 (134)	30 (91)	31 (345)
August	**mean ± std**	**10.2 ± 1.6**	**13.5 ± 2.7**	**9.8 ± 0.5**	**N/A**	**13.1 ± 2.6**	**10.8 ± 0.2**	**10.5 ± 1.0**	**12.78± 2.34**	**10.3 ± 0.3**
	range	6.7 to 16.9	9.2 to 24.0	9.2 to 12.3	N/A	8.1 to 21.0	10.7 to 11.5	9.7 to 18.8	8.8 to 19.2	9.8 to 11.3
	n = prof (obs)	30 (636)	31 (533)	29 (1347)	N/A	31 (877)	30 (30)	29 (337)	30 (153)	29 (493)
September	**mean ± std**	**9.8 ± 1.0**	**11.5 ± 1.9**	**10.2 ± 0.7**	**10.9 ± 1.6**	**11.8 ± 1.8**	**N/A**	**10.2 ± 0.4**	**11.3 ± 1.9**	**10.5 ± 0.3**
	range	8.1 to 13.2	8.8 to 19.4	8.1 to 13.0	9.2 to 14.8	8.3 to 18.4	N/A	9.7 to 11.3	8.6 to 15.8	10.2 to 10.9
	n = prof (obs)	28 (143)	29 (815)	29 (911)	7 (42)	30 (3595)	N/A	28 (162)	28 (83)	27 (53)
October	**mean ± std**	**8.3 ± 0.6**	**10.6 ± 0.6**	**10.2 ± 0.8**	**N/A**	**11.1 ± 0.9**	**N/A**	**9.7 ± 0.3**	**N/A**	**10.3 ± 0.1**
	range	6.2 to 10.2	9.0 to 11.5	8.6 to 12.0	N/A	8.8 to 4.0	N/A	8.9 to 9.9	N/A	10.1 to 10.4
	n = prof (obs)	8 (128)	30 (34)	28 (151)	N/A	30 (1705)	N/A	26 (29)	N/A	26 (47)
November	**mean ± std**	**8.7 ± 0.8**	**9.0 ± 0.5**	**8.6 ± 0.3**	**N/A**	**9.1 ± 0.4**	**8.3 ± 0.1**	**8.2 ± 0.3**	**7.9 ± 0.5**	**8.6 ± 0.4**
	range	4.9 to 9.6	6.9 to 9.9	7.4 to 9.6	N/A	7.2 to 10.2	8.1 to 8.5	7.1 to 8.6	7.2 to 8.7	7.7 to 9.4
	n = prof (obs)	26 (179)	28 (175)	29 (1296)	N/A	30 (622)	16 (32)	6 (50)	6 (6)	27 (268)
December	**mean ± std**	**6.9 ± 1.2**	**8.0 ± 0.4**	**8.7 ± 0.3**	**N/A**	**8.4 ± 0.4**	**N/A**	**8.4 ± 0.1**	**7.6 ± 0.3**	**8.3 ± 0.2**
	range	3.5 to 9.0	7.2 to 9.5	8.1 to 9.3	N/A	6.9 to 9.4	N/A	8.2 to 8.5	6.6 to 8.5	7.5 to 8.5
	n = prof (obs)	29 (85)	29 (378)	29 (288)	N/A	29 (2144)	N/A	28 (84)	30 (118)	30 (142)

Table 8. Monthly average water salinity (0 to 30 m) across nine regions in the Discovery Islands (1932 to 2015). N/A: not applicable: no data.

Month	Descriptive statistics	Bute Inlet	Eastern channels	Johnstone Strait and Discovery Passage	Loughborough Inlet	Northern Strait of Georgia	Northwestern channels	Phillips Arm, Frederic Arm and Cordero Channel	Ramsay Arm and Toba Inlet	Western channels
January	**mean ± std** range n = prof (obs)	**26.8 ± 3.1** 15.0 to 29.0 5 (38)	**28.3 ± 0.1** 28.3 to 28.4 3 (3)	**29.9 ± 0.5** 28.5 to 30.8 29 (352)	**N/A** N/A N/A	**29.02 ± 0.6** 26.9 to 30.0 29 (568)	**N/A** N/A N/A	**N/A** N/A N/A	**N/A** N/A N/A	**N/A** N/A N/A
February	**mean ± std** range n = prof (obs)	**27.9 ± 3.2** 2.8 to 29.8 30 (265)	**28.0 ± 0.8** 24.7 to 29.5 30 (274)	**30.3 ± 0.4** 29.0 to 30.8 26 (301)	**29.6 ± 0.2** 29.4 to 29.8 3 (3)	**28.8 ± 0.82** 23.5 to 30.3 29 (1039)	**N/A** N/A N/A	**N/A** N/A N/A	**27.6 ± 1.2** 24.5 to 29.2 7 (22)	**N/A** N/A N/A
March	**mean ± std** range n = prof (obs)	**27.6 ± 2.0** 18.7 to 29.8 8 (142)	**29.1 ± 0.90** 24.7 to 30.2 30 (437)	**30.1 ± 0.6** 28.4 to 31.1 29 (1168)	**NA** N/A N/A	**28.8 ± 1.0** 18.7 to 30.2 31 (887)	**N/A** N/A N/A	**29.5 ± 0.7** 24.6 to 30.2 30 (432)	**27.9 ± 1.4** 22.6 to 29.2 9 (37)	**29.5 ± 0.2** 28.9 to 30.2 30 (710)
April	**mean ± std** range n = prof (obs)	**28.4 ± 1.0** 25.7 to 30.0 30 (65)	**28.3 ± 0.60** 21.9 to 29.7 30 (2144)	**30.1 ± 0.5** 28.5 to 30.8 56 (1589)	**NA** N/A N/A	**29.0 ± 0.6** 24 to 30.2 30 (4025)	**29.3 ± 0.5** 27.5 to 29.6 29 (29)	**29.2 ± 0.2** 28.0 to 29.6 30 (340)	**29.2 ± 0.3** 28.3 to 29.5 25 (25)	**29.4 ± 0.2** 28.7 to 29.6 30 (774)
May	**mean ± std** range n = prof (obs)	**24.9 ± 7.5** 0.36 to 29.8 30 (990)	**27.9 ± 1.66** 21.4 to 29.9 29 (161)	**30.7 ± 0.3** 28.8 to 31.3 30 (3578)	**28.2 ± 4.4** 11.3 to 29.6 5 (17)	**28.6 ± 1.6** 11.7 to 30.4 29 (473)	**29.6 ± 0.3** 28.1 to 29.9 30 (91)	**29.2 ± 0.4** 27.2 to 29.6 28 (152)	**27.4 ± 2.8** 16.2 to 29.6 29 (66)	**29.3 ± 0.2** 28.8 to 29.9 30 (189)
June	**mean ± std** range n = prof (obs)	**23.7 ± 9.0** 0.04 to 29.8 30 (474)	**25.8 ± 3.30** 12.1 to 29.9 30 (448)	**29.7 ± 1.0** 23.1 to 31.2 31 (1217)	**27.1 ± 6.4** 0.94 to 29.7 29 (65)	**27.5 ± 2.0** 15.2 to 30.0 29 (3395)	**29.9 ± 0.5** 26.7 to 30.3 31 (94)	**28.4 ± 2.1** 2.3 to 29.3 30 (189)	**24.7 ± 5.5** 2.72 to 29.2 30 (144)	**29.3 ± 0.7** 16.3 to 29.8 30 (353)
July	**mean ± std** range n = prof (obs)	**23.1 ± 8.3** 0.25 to 29.4 29 (634)	**26.0 ± 1.58** 14.3 to 29.2 28 (2159)	**29.9 ± 1.0** 23.4 to 31.2 30 (850)	**28.0 ± 3.2** 11.7 to 29.9 7 (101)	**27.7 ± 1.8** 18.9 to 30.0 30 (3297)	**N/A** N/A N/A	**27.8 ± 2.0** 7.84 to 28.8 28 (132)	**27.2 ± 2.1** 20.7 to 29.1 30 (89)	**28.8 ± 0.6** 26.7 to 29.7 31 (345)
August	**mean ± std** range n = prof (obs)	**23.1 ± 9.1** 0.22 to 29.5 30 (489)	**26.6 ± 2.67** 14.1 to 29.6 31 (488)	**30.8 ± 0.8** 26.3 to 32.0 29 (1304)	**NA** N/A N/A	**26.8 ± 2.4** 17.1 to 30.3 31 (687)	**N/A** N/A N/A	**29.1 ± 1.1** 17.5 to 29.7 29 (336)	**27.0 ± 1.8** 18.4 to 28.9 30 (142)	**28.9 ± 0.5** 26.8 to 29.7 29 (467)
September	**mean ± std** range n = prof (obs)	**25.1 ± 7.3** 0.65 to 29.2 28 (120)	**27.7 ± 2.0** 15.4 to 29.3 29 (665)	**30.0 ± 0.8** 27.1 to 31.5 29 (745)	**28.3 ± 2.0** 19.4 to 29.3 7 (35)	**28.6 ± 1.0** 9.23 to 30.0 29 (3118)	**N/A** N/A N/A	**29.4 ± 0.1** 28.6 to 29.5 27 (107)	**27.1 ± 2.9** 14.2 to 29.1 28 (81)	**29.6 ± 0.1** 29.4 to 29.7 27 (53)
October	**mean ± std** range n = prof (obs)	**27.3 ± 1.8** 20.5 to 29.8 8 (119)	**27.2 ± 2.0** 24.5 to 29.1 4 (4)	**30.0 ± 1.0** 28.3 to 31.4 28 (149)	**NA** N/A N/A	**28.7 ± 0.7** 24.9 to 30.0 29 (1447)	**N/A** N/A N/A	**29.8 ± 0.1** 29.5 to 29.9 26 (30)	**N/A** N/A N/A	**30.0 ± 0.1** 29.9 to 30.2 26 (47)
November	**mean ± std** range n = prof (obs)	**28.1 ± 1.9** 19.2 to 29.5 26 (175)	**28.0 ± 0.8** 25.7 to 29.4 28 (173)	**30.4 ± 0.5** 27.0 to 31.0 28 (1269)	**N/A** N/A N/A	**28.8 ± 0.6** 24.4 to 29.7 30 (549)	**30.3 ± 0.1** 30.1 to 30.6 16 (32)	**28.7 ± 1.0** 25.1 to 29.7 6 (47)	**27.1 ± 0.9** 26.5 to 28.8 6 (6)	**29.2 ± 0.5** 26.8 to 30.0 27 (273)
December	**mean ± std** range n = prof (obs)	**28.2 ± 1.4** 21.0 to 29.6 29 (82)	**28.4 ± 0.3** 26.8 to 29.1 29 (349)	**29.4 ± 0.4** 28.9 to 31.1 29 (261)	**NA** N/A N/A	**28.7 ± 0.7** 23.4 to 30.0 29 (2053)	**N/A** N/A N/A	**39.0 ± 0.1** 28.8 to 29.3 28 (84)	**27.7 ± 1.01** 22.4 to 28.7 30 (118)	**28.9 ± 0.3** 26.7 to 29.3 30 (142)

Table 9. Monthly average dissolved oxygen (0 to 30 m) across nine regions in the Discovery Islands (1932 to 2015). N/A: not applicable: no data.

Month	Descriptive statistics	Bute Inlet	Eastern channels	Johnstone Strait and Discovery Passage	Loughborough Inlet	Northern Strait of Georgia	Northwestern channels	Phillips Arm, Frederic Arm and Cordero Channel	Ramsay Arm and Toba Inlet	Western channels
January	**mean ± std**	**250 ± 32**	**293 ± 4**	**254 ± 8**	**N/A**	**280 ± 21**	**N/A**	**N/A**	**N/A**	**N/A**
	range	205 to 291	290 to 296	243 to 264	N/A	239 to 306	N/A	N/A	N/A	N/A
	n = prof (obs)	4 (17)	2 (2)	3 (12)	N/A	4 (21)	N/A	N/A	N/A	N/A
February	**mean ± std**	**249 ± 41**	**238 ± 22**	**258 ± 17**	**237 ± 27**	**276 ± 32**	**N/A**	**N/A**	**236 ± 28**	**N/A**
	range	152 to 376	195 to 276	231 to 285	206 to 253	195 to 399	N/A	N/A	193 to 293	N/A
	n = prof (obs)	6 (82)	6 (43)	4 (13)	3 (3)	28 (540)	N/A	N/A	6 (17)	N/A
March	**mean ± std**	**285 ± 64**	**265 ± 35**	**255 ± 14**	**N/A**	**284 ± 37**	**N/A**	**221 ± 9**	**264 ± 26**	**223 ± 4**
	range	210 to 533	201 to 473	237 to 329	N/A	218 to 402	N/A	208 to 263	222 to 343	218 to 237
	n = prof (obs)	7 (100)	26 (396)	27 (161)	N/A	27 (371)	N/A	27 (112)	9 (36)	27 (54)
April	**mean ± std**	**187 ± 23**	**272 ± 59**	**250 ± 19**	**N/A**	**301 ± 50**	**N/A**	**252 ± 15**	**N/A**	**250 ± 7**
	range	149 to 211	204 to 538	204 to 301	N/A	194 to 485	N/A	239 to 370	N/A	240 to 304
	n = prof (obs)	2 (8)	28 (1703)	56 (630)	N/A	29 (3341)	N/A	28 (135)	N/A	28 (628)
May	**mean ± std**	**261 ± 62**	**292 ± 55**	**251 ± 12**	**309 ± 100**	**302 ± 65**	**261 ± 3**	**255 ± 17**	**277 ± 71**	**253 ± 2**
	range	129 to 439	177 to 401	218 to 276	212 to 571	192 to 525	258 to 278	218 to 326	178 to 451	251 to 262
	n = prof (obs)	10 (535)	7 (84)	29 (61)	5 (21)	29 (232)	28 (31)	28 (108)	7 (41)	26 (26)
June	**mean ± std**	**258 ± 54**	**246 ± 60**	**238 ± 23**	**261 ± 13**	**250 ± 46**	**253 ± 3**	**N/A**	**339 ± 51**	**244 ± 0**
	range	151 to 414	74 to 432	202 to 283	251 to 280	163 to 437	251 to 255	N/A	193 to 415	244 to 244
	n = prof (obs)	9 (337)	28 (251)	28 (129)	4 (4)	28 (2334)	2 (2)	N/A	10 (91)	1 (1)
July	**mean ± std**	**245 ± 64**	**238 ± 41**	**224 ± 13**	**297 ± 67**	**208 ± 41**	**N/A**	**204 ± 2**	**233 ± 56**	**218 ± 6**
	range	168 to 477	168 to 406	197 to 281	201 to 448	155 to 387	N/A	202 to 206	173 to 333	205 to 226
	n = prof (obs)	28 (252)	28 (1910)	28 (326)	7 (69)	28 (1233)	N/A	28 (28)	28 (30)	27 (134)
August	**mean ± std**	**218 ± 62**	**247 ± 55**	**209 ± 7**	**N/A**	**245 ± 44**	**N/A**	**237 ± 67**	**288 ± 68**	**204 ± 7**
	range	121 to 381	139 to 388	175 to 232	N/A	183 to 351	N/A	189 to 469	173 to 393	196 to 228
	n = prof (obs)	9 (230)	22 (193)	28 (145)	N/A	31 (133)	N/A	29 (93)	8 (28)	29 (307)
September	**mean ± std**	**224 ± 59**	**221 ± 45**	**190 ± 17**	**222 ± 30**	**221 ± 48**	**N/A**	**174 ± 2**	**233 ± 61**	**178 ± 12**
	range	163 to 359	157 to 469	136 to 243	194 to 286	129 to 554	N/A	168 to 185	1649 to 374	137 to 190
	n = prof (obs)	28 (92)	28 (259)	29 (494)	6 (35)	29 (2236)	N/A	27 (107)	28 (80)	27 (53)
October	**mean ± std**	**213 ± 33**	**238 ± 37**	**190 ± 18**	**NA**	**221 ± 35**	**N/A**	**177 ± 5**	**N/A**	**181 ± 0.6**
	range	166 to 291	196 to 263	166 to 228	N/A	150 to 379	N/A	174 to 192	N/A	180 to 182
	n = prof (obs)	5 (34)	3 (3)	28 (149)	N/A	29 (1160)	N/A	26 (29)	N/A	26 (47)
November	**mean ± std**	**215 ± 34**	**232 ± 37**	**187 ±18**	**N/A**	**239 ± 29**	**N/A**	**189 ± 6**	**267± 32**	**172 ± 1**
	range	171 to 314	172 to 350	162 to 260	N/A	158 to 299	N/A	180 to 196	221 to 293	170 to 175
	n = prof (obs)	26 (58)	28 (153)	28 (192)	N/A	30 (486)	N/A	5 (5)	5 (5)	27 (53)
December	**mean ± std**	**240 ± 39**	**283 ± 1**	**213 ± 20**	**N/A**	**244 ± 30**	**N/A**	**206 ± 3**	**N/A**	**221 ± 11**
	range	159 to 309	283 to 284	181 to 257	N/A	64 to 370	N/A	202 to 210	N/A	204 to 232
	n = prof (obs)	6 (45)	3 (3)	29 (259)	N/A	29 (1950)	N/A	28 (81)	N/A	30 (111)

APPENDIX B: SALINITY UNITS

Throughout this report, salinity has been reported in different units depending on when and what organization collected the data. All salinity values measured by farms are reported in ppt, which is the unit in which the data were provided.

Salinity data from oceanographic archives (profiles or moorings) require a short discussion. Salinity was historically determined by a variety of methods, usually by chemical determination of the chlorinity or by electrical conductivity measurements. In both cases the chemical determination was followed by an empirical conversion to salinity in units aimed to represent a 1/1000 mass ratio. Those empirical relations varied between laboratories and scientists, until 1978 when a practical salinity scale (known as PSS-78) was introduced. PSS-78 represented salinity values in a range that would be similar to the numerical values of previous salinity data in 1/1000 ratio, and was to be expressed without units. By 1980, PSS-78 had been officially recommended. For ranges of fresh to brackish waters (salinity values 0 to 33), tables compiled by Lewis and Perkin (1981) suggest that the difference between a practical salinity value in PSS-78 and a corresponding value obtained by previous methods could be as high as 0.4 in some configurations of algorithms and temperature. However, from 1971 onward, the algorithms gave salinity values closer to -0.1 of their PSS-78 equivalent. Since salinity values in the tables in this report are given to 1 significant digit (0.1), and the graphical resolution does not allow distinguishing variations of that magnitude or less, PSS-78 and non-PSS-78 salinity values were used interchangeably in calculations and in figures. However, caution should be used when attempting to interpret salinity variations involving post and pre-1980 data to accuracy better than 0.4. For a more detailed salinity analysis involving historical and recent data, a conversion of historical salinity data to a PSS-78 equivalent should be attempted, based on the documentation available and the Lewis and Perkins (1980) tables. However, this is not necessary for this report.

APPENDIX C: SOURCES OF DATA

OCEANOGRAPHIC ARCHIVES

Fisheries and Oceans Canada collects oceanographic data to conduct research and to generate nautical charts to ensure safe navigation on Canadian waters. Oceanographic data are collected through various methods, including mooring lines, CTD (conductivity, temperature and depth) and bottle/rosette devices for measuring temperature, salinity, dissolved oxygen, chlorophyll, nutrients and miscellaneous parameters. Data availability varies by region and time of year. The Marine Environmental Data Section (MEDS), administered by the Ocean Sciences Branch in Ottawa, archives all historical and current DFO (and previous Government departments with equivalent responsibilities) oceanographic profile data, in addition to data from other organizations. All Pacific Ocean and coastal British Columbia oceanographic profiles collected by DFO since the creation of the Institute for Ocean Sciences (IOS) in Sidney, BC, are available from the IOS, in addition to data which IOS acquired from several sources (including MEDS) during various recovery projects over the years. It is at IOS that all DFO Pacific region oceanographic data (CTD, bottle, moorings) are processed, quality controlled and archived.

Oceanographic profile data were extracted from MEDS within a polygon consisting of the Foreman et al. (2012) model domain (longitude vertices: 124.86ºW, 124.61ºW, 124.52ºW, 124.32ºW, 124.76ºW, 124.89ºW, 125.50ºW, 125.76ºW, 126.18ºW, 126.24ºW, 126.24ºW; latitude vertices:49.70ºN, 49.72ºN, 49.81ºN, 50.50ºN, 50.94ºN, 50.94ºN, 50.77ºN, 50.64ºN, 50.51ºN, 50.51ºN, 49.98ºN, 49.70ºN). Water temperature and salinity values measured from

rosette bottles during CTD casts were discarded to avoid over representation of samples collected at the same time and location. The resulting data consists of water temperature, salinity and dissolved oxygen profiles collected by various institutions which are today with DFO (Pacific Biological Station, Institute of Ocean Sciences, Center for Aquaculture and Environmental Research; 1932-2015), by the Pacific Naval Laboratory (1962, later Defence Research Establishment Pacific, now closed); the Royal Canadian Navy, Meteorological and Oceanography Centre, West Coast (1990-2012); the University of British Columbia (1951-1998); and the University of Alaska, Fairbanks (1965).

The earliest surviving digital data records of moorings deployed in the area are from 1973. Moorings consist of surface or submerged instruments connected to a wire anchored on the sea floor which measure parameters such as currents, temperature and salinity. Mooring data for temperature and salinity from moorings shallower than 60 m depth and located within the same polygon as above were acquired from the IOS file mooring repository. The resulting and available data were collected by the Canadian Hydrographic Service (1973-1978, 1987-1988) and by IOS during the World Class Tanker Safety System (2013-2014) and Ambient Monitoring (2008-2012) programs.

BC SALMON FARMERS ASSOCIATION DATABASE

As a condition of licence for marine finfish aquaculture in British Columbia, all farms must ensure that "*Environmental data associated with the facility, as set out in Appendix VI-B, must be collected and maintained at this facility and made available to a Fishery Officer or Fishery Guardian upon request*" as specified under paragraph 7.2 of the Marine Finfish Aquaculture Licence under the Fisheries Act (DFO, 2015).

Appendix VI-B is a template table specifying the environmental information to be collected at the farms. These data include: sampling date, fish health zone, facility reference number, company name, facility name, temperature between 0 and 1 m depth, temperature at 5 m depth, dissolved oxygen at 5 m depth, salinity between 0 and 1 m depth, and salinity at 5 m depth. A note section is also provided for monitoring and recording other environmental information such as occurrence of harmful algal blooms. The frequency at which the above environmental parameters must be collected is not specified. Some Atlantic Salmon farms collect more environmental data than prescribed by the conditions of licence; hence measurements are sometimes also available at 10 and 15 m depths. Standard Operating Procedures (SOPs) to meet these requirements are not mandatory, nevertheless some companies have developed SOPs which specify monitoring frequency, equipment operation, calibration and maintenance instructions.

The British Columbia Salmon Farmers' Association (BCSFA) maintains a database which includes daily environmental observations collected on Atlantic Salmon farms. Under a data sharing agreement, the BCSFA provided temperature, salinity and oxygen observations collected between 2005 and 2015. Farm raw data used in this report are confidential business information and hence not reported at the individual farm level.